Materials and methods

Reagents and antibodies. Rneasy (Qiagen), Titan One Tube RT-PCR System (Roche Molecular Biochemicals), and pGEM-T Easy Vector Systems (Promega) were purchased from individual suppliers. ABI PRISM dye terminator cycle sequencing ready kit was obtained from Perkin–Elmer. Ponasterone A (Pon A) was purchased from Invitrogen. Anti-53BP2 mouse monoclonal (BD Transduction Laboratories) and anti-tubulin mouse monoclonal (Sigma) antibodies were purchased from individual suppliers. Human kidney Total RNA was purchased from BD Biosciences.

Cell culture. 293 cells were grown at 37 °C in Dulbecco's modified Eagle's medium (DMEM; CellGro) with 10% (v/v) heat-inactivated fetal calf serum (IBL, Maebashi, Japan), 1 mM glutamate, 100 U/ml penicillin, and 100 μg/ml streptomycin. The 293/53BP2 cell line (REF), inducibly expressing 53BP2, was kindly provided by Dr. Louie Naumovski. 293/53BP2 cells were grown in DMEM with 10% (v/v) heat-inactivated fetal calf serum, 290 μg L-glutamine, 100 U/ml penicillin, 100 μg/ml streptomycin, 600 μg/ml G418, and 500 μg/ml zeocin. THP1 cells were maintained in RPMI 1640 (Sigma) with 10% heat-inactivated fetal bovine serum (IBL, Maebashi, Japan), penicillin (100 U/ml), and streptomycin (100 μg/ml). These cells were maintained in logarithmic growth at 37 °C in 5% CO_2.

RT-PCR. Total cellular RNA was prepared from each cell clone using RNeasy (Qiagen). Purification of polyadenylated mRNA was carried out using Oligotex-dT30 super RNA purification kit (Takara, Ohtsu, Japan) according to the manufacturer's instructions. The mRNA samples were digested with RNase-free DNase, ethanol precipitated, and further purified through Microcon YM-100 columns (Amicon). The quantity and quality of mRNA was assessed by capillary electrophoresis using Agilent 2100 Bioanalyzer (Agilent technologies). Approximately 1 μg of purified mRNA was used for RT-PCR using Titan One Tube RT-PCR System (Company) in which the cDNA synthesis as well as PCR was performed with reverse transcriptase, AMV, and Expand High Fidelity enzyme mix in one tube. The primer sequences were as follows: exon 1-F, forward (5′-ATG CGG TTC GGG TCC AAG ATG-3′); exon 3-F, forward (GTA GAG ATA GAG TTT CAT C-3′); exon 3-R, reverse (5′-CAC TAG AGG CTG ATC GTG G-3′); exon 4-R, reverse (5′-AAT GTC CCT GCC AGG GGG-3′); and exon 6-R, reverse (5′-GCC ATT TCC TGA AGT TCA GC-3′). The annealing temperature, 55 °C, was used for RT-PCR, except for the reaction with kidney RNA (50 °C). RT-PCR products were separated on 2.0% agarose gels and visualized by EtBr staining. All RT-PCR products were cloned to pGEM-T Easy Vector (Promega) and the nucleotide sequencing was performed with at least three individual clones by dideoxynucleotide sequencing using ABI PRISM dye terminator cycle sequencing ready kit (Perkin–Elmer Life Sciences) on an Applied Biosystems 313 automated DNA sequencer.

Western blotting. 293 and THP1 cells were harvested, washed with PBS, and lysed in 200 μl ice-cold lysis buffer (50 mM Tris–HCl, pH 8.0, 100 mM NaCl, 5 mM EDTA, 50 mM sodium fluoride, 2 mM dithiothreitol, 0.25% Nonidet P-40, 1 mM phenylmethylsulfonyl fluoride, 10 μg/ml aprotinin, 10 μg/ml leupeptin, and 1 μg/ml pepstatin A). The lysate was cleared by centrifugation and the protein concentration of the whole cell extract was measured using Bio-Rad DC protein assay kit (Bio-Rad). 293/53BP2 cells, in which 53BP2 is expressed under the ecdysone-inducible promoter, were grown to approximately 50% confluence and treated with Pon A (5 μM) for 48 h to induce 53BP2. Cells were then harvested and lysed in ice-cold lysis buffer. Supernatants (10 μg of the whole protein) were resolved by 5% SDS–PAGE and transferred on PVDF (Millipore) membrane followed by incubating with an anti-53BP2. The immunoreactive proteins were visualized by enhanced chemiluminescence (ECL) (Super Signal; Pierce).

Results

RT-PCR for TP53BP2 mRNA species

We and others have previously demonstrated that both 53BP2 and ASPP2 are encoded by a single-copy gene, TP53BP2 [2,6,9]. As shown in Fig. 1, TP53BP2 gene appears to consist of 19 exons based on the sequence information of TP53BP2 genome (Accession No. NT_004559.11) and 53BP2 cDNA (Accession No. NM_005426). Although exon 1 contains the translation start site for

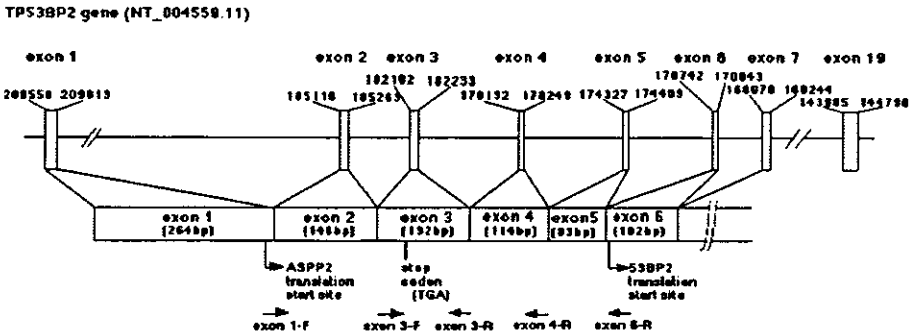

RT-PCR primers	Expected size of the products (bp)
primer set 1: "exon 1-F" and "exon 4-R"	421
primer set 2: "exon 1-F" and "exon 6-R"	554
primer set 3: "exon 3-F" and "exon 3-R"	132
primer set 4: "exon 3-F" and "exon 4-R"	246

Fig. 1. The genomic organization of the TP53BP2 gene. TP53BP2 (human genome locus ID: 7159; Accession NT_004559.11) gene, consisting of 19 exons, is found in the genomic region spanning 66,629 bp. The sequence numbers indicated for each exon are quoted from the minus strand of TP53BP2 genomic sequence (NT_004559.11). 53BP2 and ASPP2, containing 1005 and 1128 amino acids (aa), respectively, are encoded by the same gene TP53BP2 using different initiation methionine codons in the same open reading frame. The size of each exon was described within the box. Positions of primer for RT-PCR are indicated with arrows. The primer sets for RT-PCR and expected size of the products are shown in the lower panel.

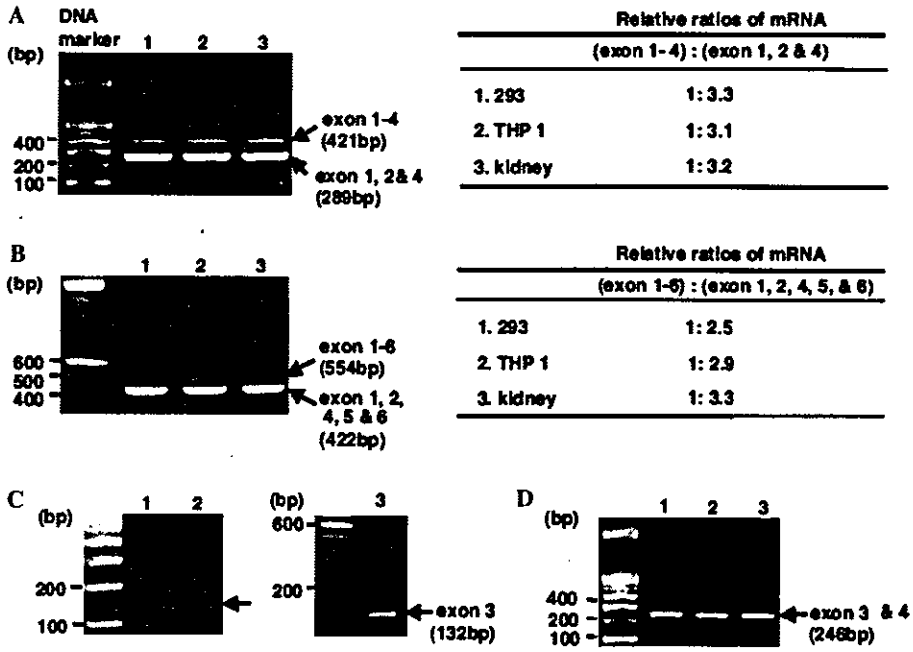

Fig. 2. The results of RT-PCR for TP53BP2 mRNA species. (A,B) RT-PCR using primer set 1 (exon 1-F and exon 4-R), and primer set 2 (exon 1-F and exon 6-R) (for locations of these primers see Fig. 1, lower panel). The right panels show the relative intensity of the products using NIH image (version 1.63) software. (C,D) RT-PCR using primer set 3 (exon 3-F and exon 3-R) and primer set 4 (exon 3-F and exon 4-R). The arrows indicate the products. The template RNAs are as follows: lane 1, mRNA from 293 cells; lane 2, mRNA from THP1 cells; and lane 3, human kidney total RNA. The 100 bp ladder DNA marker was loaded in the left lane. The size of each band of RT-PCR was confirmed by DNA sequence determination.

ASPP2, its ORF is interrupted by the stop codon located in exon 3. Whereas, the 53BP2 translation start site is located in exon 6. Thus, there are two possibilities: (i) 53BP2 and ASPP2 proteins are encoded by the same mRNA devoid of exon 3, in which two distinct translation start codons are utilized, and (ii) 53BP2 and ASPP2 proteins are encoded by distinct mRNA with or without exon 3, respectively. To address these two possibilities, we performed RT-PCR with mRNA samples prepared from 293 (human embryonal kidney) and THP1 (monocyte/macrophage) cell lines, and normal human kidney tissue using various primer sets described in Fig. 1.

We first examined if the exon 3 is transcribed into a mature mRNA. As demonstrated in Fig. 2A, RT-PCR using primer set 1 (exon 1-F and exon 4-R) yielded two bands. The intensity of each band was measured by NIH image (version 1.63) and the ratio (upper band containing exon 3: lower band not containing exon 3) was estimated to be 1:3.3, 1:3.1, and 1:3.2 in 293 cells, THP1 cells, and kidney, respectively (Fig. 2A).

To confirm the results in Fig. 2A, we performed RT-PCR using primer set 2 (exon 1-F and exon 6-R) and yielded two amplified bands (Fig. 2B). The intensity of each band was similarly measured with the ratio (the upper band:the lower band) of 1:2.5, 1:2.9, and 1:3.3 in 293 cells, THP1 cells, and kidney, respectively (Fig. 2B). Furthermore, when primer set 3 (exon 3-F and exon 3-R) and primer set 4 (exon 3-F and exon 4-R) were used, only a single band was detected in each reaction (Figs. 2C and D).

DNA sequence analysis of RT-PCR products of TB53BP2 mRNA species

All DNA fragments of RT-PCR products have been isolated, cloned into pGEM-T Easy Vector, and the nucleotide sequences were determined. As shown in Fig. 3, the DNA sequence analysis clearly indicated that the upper band in Fig. 2A contained exons from 1 to 4 (421 bp) and the lower band contained exons from 1 to 4 but not exon 3 (289 bp). The upper band in Fig. 2B contained exons from 1 to 6 (554 bp), whereas the lower band contained exons from 1 to 6, but not exon 3 (422 bp) (data not shown). The single band seen in Figs. 2C and D contained exon 3 (data not shown). Thus, we concluded that exon 3 is actually transcribed in some, but not all, mRNA species encoded by TP53BP2 gene. These results indicated that TP53BP2 gene encodes two distinct mRNA species with or without exon 3 by alternate splicing in various cells and tissues.

Western blotting

To confirm the above results, we examined the expression of 53BP2 proteins by Western blotting. As demonstrated in Fig. 4, two proteins of 137 and 150 kDa

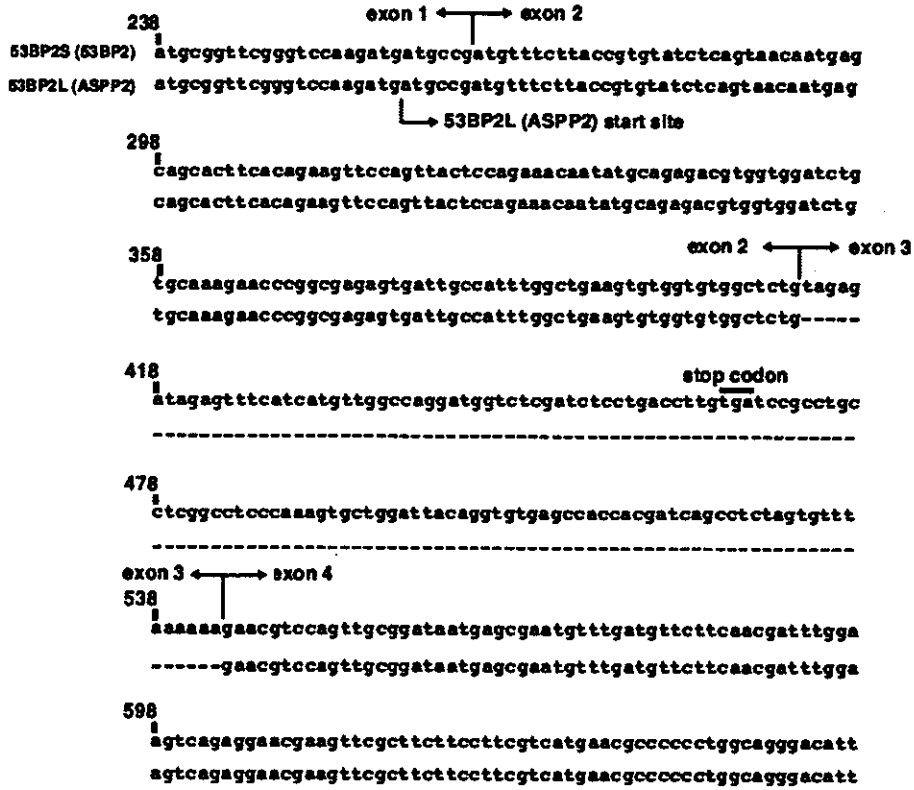

Fig. 3. DNA sequence of RT-PCR products of TB53BP2 mRNA splicing variants. The alignment of DNA sequences of the 421 and 289 bp RT-PCR products obtained with primer set 1 (exon 1-F and exon 4-R) (Fig. 2) is shown here. These splicing variants are named as 53BP2S (short) and 53BP2L (long). Whereas 53BP2S mRNA contains exons 1–4, 53BP2L (previously called ASPP2) contains exons 1–4, but not exon 3.

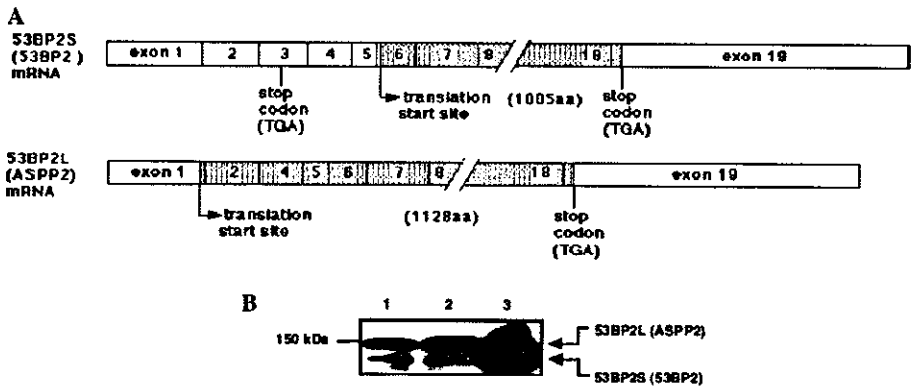

Fig. 4. Detection of two 53BP2 proteins by Western blotting. (A) Subgenomic organization of 53BP2 mRNA species. 53BP2S mRNA consists of exons 1–19, whereas 53BP2L (ASPP2) mRNA contains exons 1–19, but not exon 3. Open reading frames of these 53BP2 proteins are indicated by shadowed boxes. (B) Detection of 53BP2 proteins. The whole protein samples were prepared from 293 cells (lane 1), THP1 cells (lane 2), and 293/53BP2 cells (lane 3) expressing 53BP2 (1005 aa) [4] as a positive control. Each sample (10 μg of the whole protein) was resolved by 5% SDS–PAGE and transferred on PVDF membrane followed by incubating with an anti-53BP2 mouse monoclonal antibody followed by chemiluminescence detection. The protein marker was loaded in the left lane and the position of 150 kDa protein marker is indicated. The exposure of chemiluminescence for protein detection revealed the endogenous 53BP2S (formerly "53BP2") (the lower band) and 53BP2L (formerly "ASPP2") (the upper band) proteins in these cells. The similar results were obtained in the repeated experiments.

corresponding to formerly called 53BP2 and ASPP2 proteins, respectively, are detected in both 293 and THP1 cells. The relative amounts of 53BP2 versus ASPP2 proteins were approximately 1:3 consistent with the relative amounts of their mRNA species. As these proteins are expressed from the same gene by alternative splicing, we propose to call these proteins as 53BP2S (short) and 53BP2L (long), containing 1005 aa (derived from all exons of TP53BP2) and 1128 aa (derived from TP53BP2 mRNA devoid of exon 3), respectively.

Discussion

53BP2 has been identified initially as one of the interacting proteins of p53 and has been implicated in carcinogenesis. The 53BP2 binding site on the p53 core domain consists of evolutionarily conserved regions that are frequently mutated in human cancer [3,11] and the level of TP53BP2 mRNA expression in various human cancer cell lines was correlated with the sensitivity to DNA damaging agents [7], indicating that this protein may play an important role in carcinogenesis and its progression. However, no TP53BP2 mutation was detected in various cancer cell lines [7]. With regard to the structural property of the p53–53BP2 complex, Gorina and Pavletich [3] reported the crystal structure of the p53 core domain bound to the 53BP2 protein, which revealed that (i) the SH3 domain located in the C-terminus of 53BP2 binds the L3 loop of p53 which is responsible for the sequence-specific DNA binding activity of p53, and (ii) the ankyrin repeat of 53BP2 binds the H1 helix of p53 which is required for the p53 homodimerization. Thus, when p53-53BP2 complex forms in vivo, p53 is not able to bind to DNA.

The proapoptotic action of 53BP2 proteins has been well established [4–6,10]. Two possibilities are entertained to explain this action of 53BP2 proteins. First, Samuels-Lev et al. [10] reported that 53BP2L (ASPP2) specifically enhance p53-induced apoptosis by enhancing the DNA binding and transactivation function of p53 on the promoters of proapoptotic genes, such as Bax in vivo, although the nuclear localization of this protein was not clearly demonstrated. However, as mentioned above, the crystal structure studies of p53–53BP2 complex did not support this possibility since p53, once bound to 53BP2, is no longer able to form p53 homodimer but also to bind to DNA. Second, Yang et al. [6] showed that 53BP2 is predominantly located in cytoplasm and transiently in mitochondria. In addition, we have recently confirmed the mitochondrial translocalization of 53BP2 concomitantly with its proapoptotic action and the specific activation of caspase-9 but not caspase-8 (Kobayashi, Takahashi, and Okamoto, submitted). Interestingly, Mihara et al. [12] demonstrated using cell fractionation and electromicroscopic examinations that p53 is located in mitochondria during p53-induced apoptosis upon DNA damage. Therefore, it is interesting to examine if 53BP2 interacts with p53, locates to mitochondria, and induces apoptosis through mitochondrial death pathway. Since there is no characteristic protein motif in the N-terminal 123 aa region of 53BP2L (ASPP2) as far as we searched, these proteins seem to have a similar biological action although we do not currently know the reason for such redundancy.

In addition to the 53BP2 involvement in carcinogenesis, it may also be involved in autoimmunity. Tsao et al. [13] demonstrated a number of genetic loci associated with the familial incidence of systemic lupus erythematosus including one corresponding to 1q42.1, which is the same chromosomal locus assigned to TP53BP2 [9]. We have also shown that overexpression of p65 subunit of NF-κB prevents the cell death induced by 53BP2 [6] by binding to 53BP2. Therefore, in the sporadic cases of systemic lupus erythematosus, aberrant activation of NF-κB such as in the developing thymus may perturb the 53BP2-mediated apoptosis of the self-reactive lymphocyte clones.

Acknowledgments

This work was supported by Grants-in-Aid from Ministry of Education, Culture, Sports, Science and Technology (Grant No.14028052), and Japan Human Sciences Foundation (Grant No. SA14721).

References

[1] K. Iwabuchi, P.L. Bartel, B. Li, R. Marraccino, S. Fields, Proc. Natl. Acad. Sci. USA 91 (1994) 6098–6102.
[2] L. Naumovski, L.M. Cleary, Mol. Cell. Biol. 16 (1996) 3884–3892.
[3] S. Gorina, P.N. Pavletich, Science 274 (1996) 1001–1005.
[4] Y. Ao, H.L. Rochde, L. Naumovski, Oncogene 20 (2001) 2720–2725.
[5] D.C. Lopez, Y. Ao, H.L. Rohde, D.T. Perez, J.D. O'Connor, X. Lu, M.J. Fors, L. Naumovski, Mol. Cell. Biol. 20 (2000) 8018–8025.
[6] P.J. Yang, M. Hori, N. Takahashi, T. Kawabe, H. Kato, T. Okamoto, Oncogene 18 (1999) 5177–5186.
[7] T. Mori, H. Okamoto, N. Takahashi, R. Ueda, T. Okamoto, FEBS Lett. 465 (2000) 124–128.
[8] A.E. Slee, X. Lu, Toxicol. Lett. 139 (2003) 81–87.
[9] P.J. Yang, T. Ono, S. Sonta, T. Kawabe, T. Okamoto, Cytochem. Cell Genet. 78 (1997) 61–62.
[10] Y. Samuels-Lev, J.D. O'Connor, D. Bergamaschi, G. Trigiante, K.J. Hsieh, S. Zhong, I. Campargue, L. Naumovski, T. Crook, X. Lu, Mol. Cell 8 (2001) 781–794.
[11] K. Iwabuchi, B. Li, F.H. Massa, J.B. Trask, T. Date, S. Field, J. Biol. Chem. 273 (1998) 26061–26068.
[12] M. Mihara, A. Erster, A. Zaika, O. Petrenko, T. Chittenden, P. Pancoska, U. Moll, Mol. Cell 11 (2003) 577–590.
[13] T.B. Tsao, M.R. Cantor, C.K. Kalunian, C.-J. Chen, H. Badsha, R. Singh, J.D. Wallace, C.R. Kitridou, S.-I. Chen, N. Shen, W.Y. Song, A.D. Senberg, C.-L. Yu, H.B. Hahn, I.J. Rotter, J. Clin. Invest. 99 (1997) 275–731.

International Immunology, Vol. 16, No. 1, pp. 163–168
doi: 10.1093/intimm/dxh013

Molecular genetic analyses of human *NKG2C* (*KLRC2*) gene deletion

Risa Miyashita[1], Naoyuki Tsuchiya[1], Koki Hikami[1], Kimiko Kuroki[1], Toru Fukazawa[2], Marc Bijl[3], Cees G. M. Kallenberg[3], Hiroshi Hashimoto[2], Toshio Yabe[4] and **Katsushi Tokunaga[1]**

[1]Department of Human Genetics, Graduate School of Medicine, University of Tokyo, Tokyo 113-0033, Japan
[2]Department of Rheumatology and Internal Medicine, Juntendo University, Tokyo 113-8421, Japan
[3]University Hospital Groningen, 9713 GZ Groningen, The Netherlands
[4]Tokyo Metropolitan Red Cross Blood Center, Tokyo 150-0012, Japan

Keywords: genome, NK cell, polymorphism, rheumatoid arthritis, systemic lupus erythematosus

Abstract

Human *NKG2A*, *NKG2C* and *NKG2E* genes are located on 12p13 in the NK gene complex. We recently identified deletion of *NKG2C* in a Japanese population. This study was performed to identify the breakpoint, and to examine the association of *NKG2C* deletion with susceptibility to rheumatoid arthritis and systemic lupus erythematosus. The location of the breakpoint was determined to be 1.5–1.8 kb telomeric from the 3′ end of *NKG2A* by comparing sequences of the intergenic segments upstream and downstream of the *NKG2C* gene in the common haplotype with the intergenic sequence between *NKG2A* and *NKG2E* in the deletion haplotype. Based on this information, a genotyping system was developed. The frequency of *NKG2C* deletion haplotype was 20.2% in Japanese and 20.0% in Dutch populations. The frequency of homozygous deletion was 4.1% in Japanese and 3.8% in Dutch. Evidence for an association with rheumatic diseases was not detected. These results indicated that *NKG2C* deletion is commonly present in Japanese and Dutch, suggesting that *NKG2C* is not essential for survival and reproduction, and is not associated with rheumatic diseases.

Introduction

Human NK cells are regulated by opposing signals from HLA class I receptors of two distinct families, the Ig superfamily and the C-type lectin superfamily, that activate or inhibit effector functions (1–5). Imbalance of such signals may possibly be involved in the pathogenesis of autoimmune diseases such as rheumatoid arthritis (RA) and systemic lupus erythematosus (SLE).

Human NKG2 molecules belong to the C-type lectin family. To date, seven members including splicing isoforms have been identified (6–9). Among the NKG2 family, NKG2C and NKG2E are expressed as heterodimers with CD94. Upon contacting HLA-E (10), they deliver activating signals via adaptor molecules such as DAP12 (11). *NKG2* genes are located on chromosome 12p13 in the NK gene complex (NKC) (12,13), one of the candidate susceptibility regions of RA and SLE identified by linkage analyses (14–16). Although only suggestive evidence for linkage with RA and SLE with 12p13 has been reported, the detection power of the linkage analyses is highly limited in the case of complex diseases, where each susceptibility gene is assumed to confer modest to moderate relative risk (18,19). In fact, disease-associated polymorphisms have often been identified by association studies in chromosomal regions where only modest or no linkage was demonstrated (19). For example, association of mannose-binding lectin polymorphisms with SLE has been repeatedly reported, in spite of absence of significant linkage [reviewed in (20)]. Since NK cells have been functionally implicated in rheumatic diseases (21), genetic association with disease susceptibility needs to be examined at least for the polymorphisms with potential functional relevance.

In a previous study, in the process of variation screening of *NKG2* genes, we found that a proportion of the Japanese population lacks the *NKG2C* gene (also designated as *KLRC2*), due to homozygous deletion of an ~16-kb genomic region encompassing *NKG2C* (17).

Correspondence to: N. Tsuchiya; E-mail: tsuchiya-tky@umin.ac.jp

Transmitting editor: W. M. Yokoyama

Received 12 August 2003, *accepted* 9 October 2003

To establish a genotyping system and to determine the frequency of the *NKG2C* deletion haplotype, it was essential to map the precise breakpoint. In the present study, we attempted to identify the breakpoint, to determine the frequency of the *NKG2C* deletion haplotype, and to examine its association with susceptibility to RA and SLE, in Japanese and Dutch populations.

Methods

Subjects

Genotyping was performed using the genomic DNA from 245 healthy Japanese (mean age 32.9 ± 9.4 years) and 105 healthy Dutch individuals. For the case-control association studies, 174 Japanese patients with RA (58.3 ± 11.1 years), and 155 Japanese (41.3 ± 14.1 years) and 89 Dutch patients with SLE (44.8 ± 14.4 years) were also genotyped. Diagnoses of RA, SLE and the classification for the presence of lupus nephritis were based on the American College of Rheumatology criteria (22,23). The subjects were recruited in Tokyo and Groningen respectively. This study was approved by the Institutional Review Boards of the participating institutions.

Determination of the breakpoint

The location of the breakpoint was determined by comparing sequences of the intergenic segments upstream and downstream of the *NKG2C* gene in the common haplotype with the intergenic sequence between *NKG2A* (*KLRC1*) and *NKG2E* (*KLRC3*) in the deletion haplotype. High-mol.-wt genomic DNA was isolated from the peripheral blood from individuals previously determined to be homozygous for the common or the deletion type (17), using the Puregene DNA isolation kit (Gentra Systems, Minneapolis, MN).

To amplify the intergenic segment upstream of the *NKG2C* in the common haplotype, primers were placed within the 3′-untranslated region (3′UTR) of *NKG2A* and the promoter region of *NKG2C*. The forward and reverse primers were NKG2C1 (5′-GCATTTGCAGTGCATCAGATAAATTG-3′) and NKG2C2 (5′-CGGTTCCTTCTCTAATCATGACTTATTGTCTA-3′) respectively. The primers to amplify the intergenic segment downstream of the *NKG2C* in the common haplotype were placed within the 3′UTR of *NKG2C* and the promoter region of *NKG2E*. The forward and reverse primers were NKG2C3 (5′-TTGCGTTTACAGTGCATCAGATACATTT-3′) and NKG2C4 (5′-GGTTCCTTCTCTAATCATGACTTACTGTCTG-3′) respectively. In the sample homozygous for the deletion haplotype, primers NKG2C1 and NKG2C4 were used to amplify the intergenic segment between *NKG2A* and *NKG2E* of the deletion haplotype. Each reaction was performed using the Takara LA Taq kit (Takara, Otsu, Japan). The PCR condition consisted of initial denaturation at 96°C for 10 min, followed by 35 cycles of denaturation at 96°C for 30 s, annealing at 66.5°C for 30 s and extension at 72°C for 10 min. The sequences were then determined by direct sequencing using commercial reagents (ABI Prism dRhodamine Terminator Cycle Sequencing-Ready Reaction kit; Applied Biosystems, Foster City, CA).

Genotyping for the deletion haplotype

The principle of the genotyping method is described later in the Results. The primers for PCR#1 were BREAK-F (5′-ACTCGGATTTCTATTTGATGC-3′) and BREAK-R (5′-ACA-AGTGATGTATAAGAAAAAG-3′). The PCR condition consisted of initial denaturation at 96°C for 10 min, followed by 35 cycles of denaturation at 96°C for 30 s, annealing at 54°C for 30 s and extension at 72°C for 40 s. The primers for PCR#2 were NKG2CT/F (5′-ATCAATTATTGAAATAGGATGC-3′) and NKG2CT/R (5′-CGCAAAGTTACAACCATCACCAT-3′). PCR was performed similarly for 27 cycles with the annealing temperature at 57°C. The primers for NKG2A (internal control) were NKG2A3F (5′-TGTATCCACCTCTCCTTTCG-3′) and NKG2A4R (5′-TTTGTACAGCCTAAGATCAAG-3′) (17). The diplotype frequencies were compared between patients and healthy individuals using χ^2-test at the significance level of 5%.

Linkage disequibrium (LD) analysis

Eight polymorphisms previously described in the *NKG2A* gene and one in the *CD94* gene (17) were analyzed for the LD with *NKG2C* deletion in the 177 Japanese healthy individuals. The polymorphisms analyzed were: c.−169G → A, c.−31A → G, c.238T → A, c.284–67_–62delAAACTT, c.338–90A → G, c.1015C → T, c.1077C → T and c.1146_1150delGATTT of *NKG2A*, and c.−134A → T of *CD94*. The extent of LD was assessed by Lewontin's *D′* (24), using the software package SNPalyze version 2.2 (Dynacom, Tokyo, Japan).

Results

Determination of the breakpoint of the NKG2C deletion

The intergenic segments upstream and downstream of the *NKG2C* gene were highly homologous (Figs 1 and 2a); therefore, scattered nucleotide substitutions that characterize each sequence were used to determine the location of the breakpoint. The centromeric portion of the intergenic sequence of the deletion haplotype was identical with that of the corresponding region of the upstream segment of the *NKG2C* in the common haplotype, while the telomeric portion of the intergenic sequence of the deletion haplotype was identical with the downstream segment of the *NKG2C* in the common haplotype. The breakpoint was found to be within the 292-bp region 1.5–1.8 kb telomeric from the 3′UTR of *NKG2A*. Around the breakpoint, several nucleotides unique to the deletion haplotype were observed.

Genotyping for the NKG2C deletion haplotype

Based on these findings, we developed a typing system for the *NKG2C* deletion. The diplotype for the presence or absence of *NKG2C* was determined by the combination of two sets of PCR (Fig. 2a). In PCR#1, the primers were placed at both sides of the breakpoint. Amplification of a 411-bp fragment is observed only in the presence of the *NKG2C* deletion. In PCR#2, the primers were placed within exon 6 of *NKG2C* to detect the presence of the common haplotype. Amplification of a 363-bp fragment is observed only in the presence of *NKG2C*. When amplification was observed both in PCR#1 and #2, the subject was typed as heterozygous for the deletion (Fig. 2b).

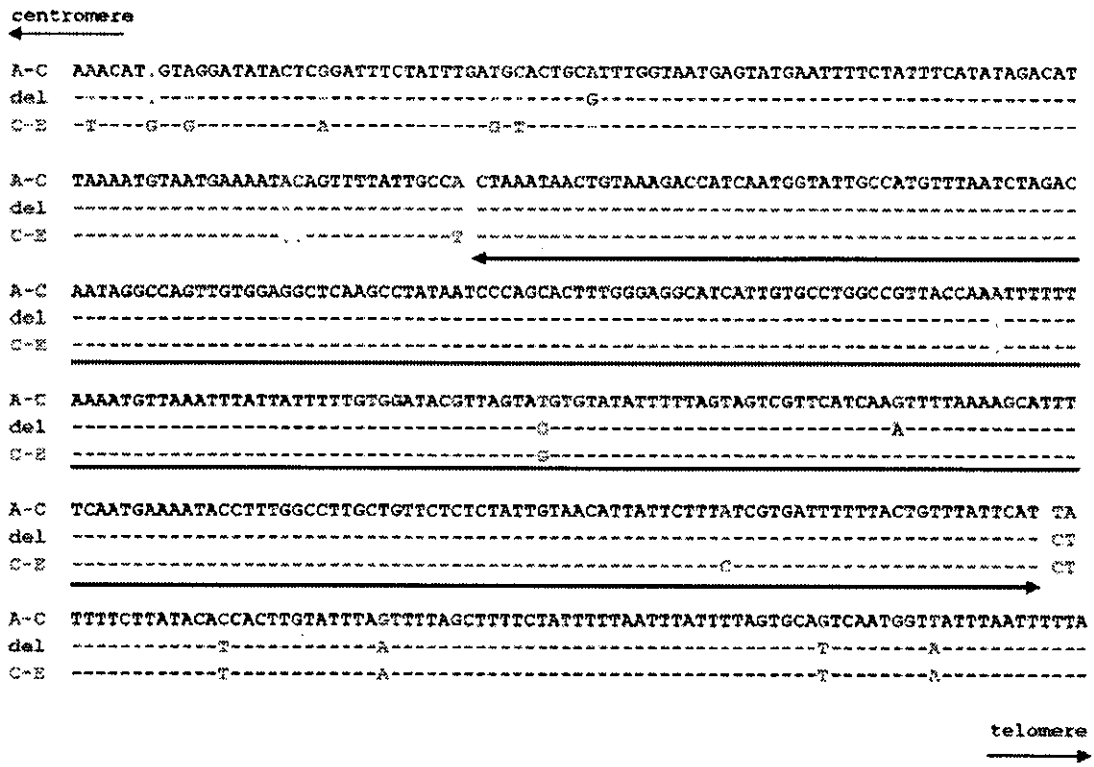

Fig. 1. Determination of the breakpoint. The intergenic sequences upstream of *NKG2C* (upper) and downstream of *NKG2C* (lower) were compared with the intergenic sequence of a deletion haplotype (middle). Only the sequences around the breakpoint are shown. Dashes denote identity with the intergenic segments upstream and downstream of *NKG2C*, and dots indicate insertions/deletions. For the positions at which the nucleotides differ between intergenic segments upstream and downstream of *NKG2C*, identity is shown in red and green respectively. The breakpoint was determined to be within the 292-bp segment shown by the bidirectional arrow. Two nucleotides shown in blue were present only on the deletion haplotype, but were common in Japanese and Dutch subjects, suggesting that these nucleotide substitutions accumulated after the *NKG2C* deletion event, but before the divergence of Asian and Caucasian populations.

Using this system, the diplotype frequencies in the Japanese and Dutch populations were determined (Table 1). Approximately 4% of the general population lacks *NKG2C*.

The frequency of the *NKG2C* deletion haplotype was remarkably similar in both populations: 20.2% in Japanese and 20.0% in Dutch. Significant association with the susceptibility to SLE and RA (Table 1) or with lupus nephritis (data not shown) was not observed.

LD analysis

To elucidate the extent of the haplotype block that contains the *NKG2C* deletion, LD with eight *NKG2A* polymorphisms described in the previous paper (17) were examined. Only the two polymorphisms in the 3′UTR (c.1077C → T and c.1146_1150delGATTT) showed strong LD with the *NKG2C* deletion ($D' > 0.9$), while the remainder showed only modest to moderate LD ($D' < 0.6$), indicating that the centromeric boundary of the haplotype containing the *NKG2C* deletion is within the *NKG2A* locus. Similarly, only weak LD was observed between the *NKG2C* deletion and *CD94* c.−134A → T ($D' = 0.19$).

Discussion

In this study, we identified the breakpoint of the human *NKG2C* gene deletion, which we recently found to be commonly present in the general population (17). By comparing the genomic sequences between *NKG2A* and *NKG2E*, the breakpoint was determined to be 1.5–1.8 kb telomeric from the 3′ end of *NKG2A*. *NKG2* genes are postulated to have developed through gene duplication events and several *Alu* repeats are present in this region (25,26). The *NKG2C* deletion is most likely a result of an unequal crossover event; however, although *Alu* repeats are often involved in gene recombination events (27), the breakpoint of the *NKG2C* deletion was not located in the *Alu* sequence.

Around the breakpoint, several nucleotides unique to the deletion haplotype were present, suggesting that these nucleotide substitutions have occurred after the divergence of this haplotype. Interestingly, direct sequencing revealed that the nucleotides unique to the deletion haplotype were shared among Japanese and Dutch individuals, suggesting that the *NKG2C* deletion haplotype in these populations is a result of a common ancestral event. LD analysis demonstrated

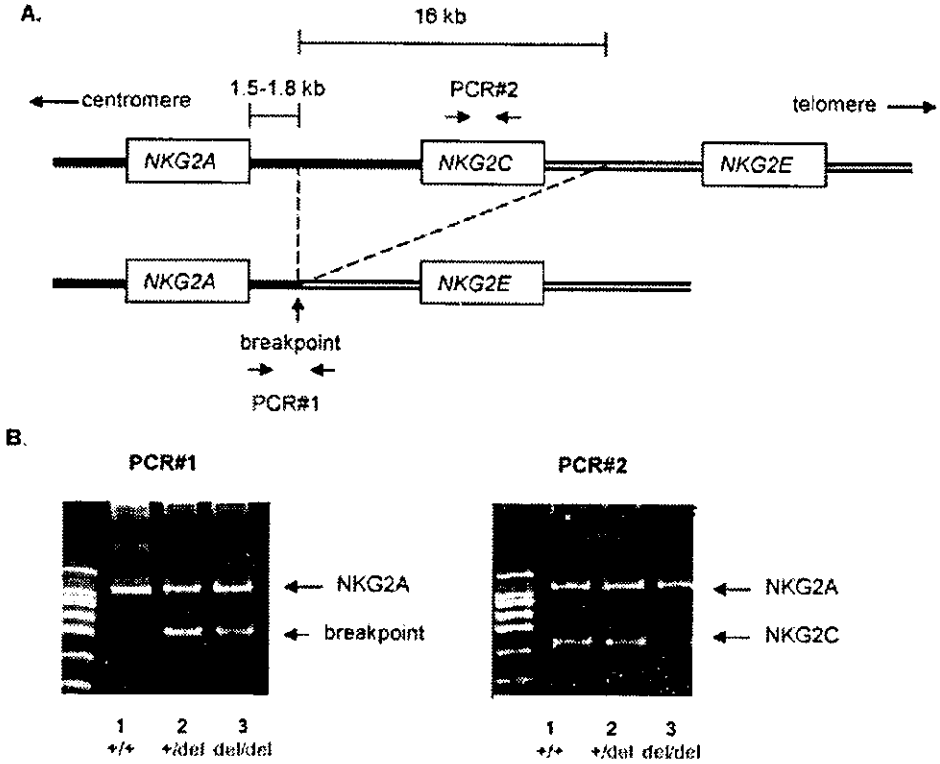

Fig. 2. (A) The position of the breakpoint and the strategy for the *NKG2C* deletion genotyping. The breakpoint was mapped to the 1.5–1.8 kb telomeric region from the 3'UTR of *NKG2A*. The diplotype for the presence or absence of *NKG2C* was determined by the combination of two sets of PCR. In PCR#1, the primers were placed at both sides of the breakpoint. Amplification of a 411-bp fragment is observed only in the presence of the *NKG2C* deletion. In PCR#2, the primers were placed within exon 6 of *NKG2C* to detect the presence of the common haplotype. Amplification of a 363-bp fragment is observed only in the presence of *NKG2C*. As an internal control, primers that amplify the 780-bp fragment of *NKG2A* exon 3 and exon 4 were used in both reactions. (B) Genotyping for *NKG2C* deletion haplotype. The diplotype of each individual was determined by using PCR#1 and #2 in combination. Lane 1, common type homozygote (+/+); lane 2, heterozygote (+/del); lane 3, deletion homozygote (del/del). Molecular weight marker used was a 100-bp ladder.

Table 1. Diplotype frequency of the *NKG2C* deletion in the Japanese and Dutch patients and controls

Japanese patients and healthy individuals	Healthy (n = 245)	SLE (n = 155)	RA (n = 176)
+/+	156 (63.7)	93 (60.0)	108 (61.4)
+/del	79 (32.2)	54 (34.8)	59 (33.5)
del/del	10 (4.1)	8 (5.2)	9 (5.1)
Dutch patients and healthy individuals	**Healthy (n = 105)**	**SLE (n = 89)**	
+/+	67 (63.8)	50 (60.0)	
+/del	34 (32.4)	34 (38.2)	
del/del	4 (3.8)	5 (5.6)	

Percentages are shown in parentheses. Statistically significant difference was not observed. Diplotype frequencies of healthy individuals were compatible with the Hardy–Weinberg equilibrium in both populations.

that the centromeric boundary of the haplotype containing the *NKG2C* deletion lies within the *NKG2A* gene and the telomeric boundary does not extend to the *CD94* gene, located 110 kb apart from *NKG2C*. Whether the *NKG2C* deletion haplotype is in LD with *NKG2E* or *NKG2D* polymorphisms needs to be examined in future studies.

We established a genotyping method for the *NKG2C* deletion, and determined the frequencies of the *NKG2C* deletion haplotype in Japanese and Dutch populations, which turned out to be remarkably similar in both populations. Although the functional consequences of the *NKG2C* deficiency remain unclear, the fact that ~4% of the general

population lacks *NKG2C* indicates that *NKG2C* is not essential for survival and reproduction. It is conceivable that lack of *NKG2C* is compensated by other activating receptors, possibly *NKG2E* (or its alternatively spliced form *NKG2H*). Such a possibility is supported by the fact that human *NKG2C* and *NKG2E* genes are highly homologous across the carbohydrate recognition domain (92% nucleotide and 90% amino acid by BLAST search), where ligand interactions would occur. In addition, a previous study that reported the normal function and number of NK cells in patients with *DAP12* deficiency suggests 'functional redundancy or developmental compensation in target recognition by NK cells' (28).

In the chimpanzee genome, two *NKG2C* genes (*Pt-NKG2CI* and *Pt-NKG2CII*) are present, which are equally diverged from human *NKG2C*. In contrast with other genes in the NKC, *NKG2C* and *NKG2E* have the highest interspecies divergence, and are also polymorphic within each species (29,30). These data suggest that *NKG2C* has evolved under relatively weak selection pressures. Our present data indicating the frequent occurrence of the *NKG2C* deletion in the general population support this possibility. On the other hand, unlike killer cell Ig-like receptors or leukocyte Ig-like receptors (also referred as Ig-like transcripts), *NKG2C* is conserved among mammalian species from mice to humans, suggesting an essential role throughout mammalian evolution. It should be noted, however, that there may be differences in the expression pattern of the NKG2 receptors between human and mice (31–33), and therefore, although the orthologous genes exist in both species, their functional roles may differ.

Further studies on population genetics, especially on possible associations with susceptibility to viral infections or cancers, as well as on functional consequences are necessary to gain insight into the significance of *NKG2C* deletion.

Acknowledgements

This work was supported by a Grant-in-Aid for Scientific Research on Priority Areas (C) 'Medical Genome Science' and Grants-in-Aid for Scientific Research (B) from the Ministry of Education, Science, Sports and Culture of Japan.

Abbreviations

DAP	DNAX-activation protein
KLRC	killer cell lectin-like receptor, subfamily C
LD	linkage disequilibrium
NKC	NK gene complex
NKG2	NK cell group 2 subfamily
RA	rheumatoid arthritis
SLE	systemic lupus erythematosus
UTR	untranslated region

References

1 Lanier, L. L. 1998. NK cell receptors. *Annu. Rev. Immunol.* 16:359.
2 Raulet, D. H., Vance, R. E. and McMahon, C. W. 2001. Regulation of the natural killer cell receptor repertoire. *Annu. Rev. Immunol.* 19:291.
3 Trowsdale, J., Barten, R., Haude, A., Stewart, C. A., Beck, S. and Wilson, M. J. 2001. The genomic context of natural killer receptor extended gene families. *Immunol. Rev.* 181:20.
4 Borrego, F., Kabat, J., Kim, D. K., Lieto, L., Maasho, K., Pena, J., Solana, R. and Coligan, J. E. 2002. Structure and function of major histocompatibility complex (MHC) class I specific receptors expressed on human natural killer (NK) cells. *Mol. Immunol.* 38:637.
5 Yokoyama, W. M. and Plougastel, B. F. 2003. Immune functions encoded by the natural killer gene complex. *Nat. Rev. Immunol.* 3:304.
6 Houchins, J. P., Yabe, T., McSherry, C. and Bach, F. H. 1991. DNA sequence analysis of NKG2, a family of related cDNA clones encoding type II integral membrane proteins on human natural killer cells. *J. Exp. Med.* 173:1017.
7 Yabe, T., McSherry, C., Bach, F. H., Fisch, P., Schall, R. P., Sondel, P. M. and Houchins, J. P. 1993. A multigene family on human chromosome 12 encodes natural killer-cell lectins. *Immunogenetics* 37:455.
8 Plougastel, B. and Trowsdale, J. 1997. Cloning of NKG2-F, a new member of the NKG2 family of human natural killer cell receptor genes. *Eur. J. Immunol.* 27:2835.
9 Belton, T., Heredia, A. B., Llano, M., Minguela, A., Rodriguez, A., Lopez-Botet, M. and Aparicio, P. 1999. Triggering of effector functions on a CD8+ T cell clone upon the aggregation of an activatory CD94/kp39 heterodimer. *J. Immunol.* 162:3996.
10 Braud, V. M., Allan, D. S., O'Callaghan, C. A., Soderstrom, K., D'Andrea, A., Ogg, G. S., Lazetic, S., Young, N. T., Bell, J. I., Phillips, J. H., Lanier, L. L. and McMichael, A. J. 1998. HLA-E binds to natural killer cell receptors CD94/NKG2A, B and C. *Nature* 391:795.
11 Lanier, L. L., Corliss, B., Wu, J. and Phillips, J. H. 1998. Association of DAP12 with activating CD94/NKG2C NK cell receptors. *Immunity* 8:693.
12 Suto, Y., Yabe, T., Maenaka, K., Tokunaga, K., Tadokoro, K. and Juji, T. 1997. The human natural killer gene complex (NKC) is located on chromosome 12p13.1–p13.2. *Immunogenetics* 46:159.
13 Plougastel, B. and Trowsdale, J. 1998. Sequence analysis of a 62-kb region overlapping the human KLRC cluster of genes. *Genomics* 49:193.
14 Jawaheer, D., Seldin, M. F., Amos, C. I., Chen, W. V., Shigeta, R., Monteiro, J., Kern, M., Criswell, L. A., Albani, S., Nelson, J. L., Clegg, D. O., Pope, R., Schroeder, H. W., Jr, Bridges, S. L., Jr, Pisetsky, D. S., Ward, R., Kastner, D. L., Wilder, R. L., Pincus, T., Callahan, L. F., Flemming, D., Wener, M. H. and Gregersen, P. K. 2001. A genomewide screen in multiplex rheumatoid arthritis families suggests genetic overlap with other autoimmune diseases. *Am. J. Hum. Genet.* 68:927.
15 Cornelis, F., Faure, S., Martinez, M., Prud'homme, J. F., Fritz, P., Dib, C., Alves, H., Barrera, P., de Vries, N., Balsa, A., Pascual-Salcedo, D., Maenaut, K., Westhovens, R., Migliorini, P., Tran, T. H., Delaye, A., Prince, N., Lefevre, C., Thomas, G., Poirier, M., Soubigou, S., Alibert, O., Lasbleiz, S., Fouix, S., Bouchier, C., Liote, F., Loste, M-N, Lepage, V., Charron, D., Gyaphy, G., Lopez-Vaz, A., Kuntz, D., Bardin, T. and Weissenbach, J. for ECRAF. 1998. New susceptibility locus for rheumatoid arthritis suggested by a genome-wide linkage study. *Proc. Natl Acad. Sci. USA* 95:10746.
16 Moser, K. L., Neas, B. R., Salmon, J. E., Yu, H., Gray-McGuire, C., Asundi, N., Bruner, G. R., Fox, J., Kelly, J., Henshall, S., Bacino, D., Dietz, M., Hogue, R., Koelsch, G., Nightingale, L., Shaver, T., Abdou, N. I., Albert, D. A., Carson, C., Petri, M., Treadwell, E. L., James, J. A. and Harley, J. B. 1998. Genome scan of human systemic lupus erythematosus: evidence for linkage on chromosome 1q in African-American pedigrees. *Proc. Natl Acad. Sci. USA* 95:14869.
17 Hikami, K., Tsuchiya, N., Yabe, T. and Tokunaga, K. 2003. Variations of human killer cell lectin-like receptors: common occurrence of NKG2-C defetion in the general population. *Genes Immun.* 4:160.
18 Risch, N. J. 2000. Searching for genetic determinants in the new millennium. *Nature* 405:847.
19 Tsuchiya, N., Ohashi, J. and Tokunaga, K. 2002. Variations in immune response genes and their associations with multifactorial immune disorders. *Immunol. Rev.* 190:169.
20 Kelly, J. A., Moser, K. L. and Harley, J. B. 2002. The genetics of systemic lupus erythematosus: putting the pieces together. *Genes Immun.* 3(Suppl. 1):S71.

21 Seaman, W. E. 2000. Natural killer cells and natural killer T cells. *Arthritis Rheum.* 43:1204–17.
22 Arnett, F. C., Edworthy, S. M., Bloch, D. A., McShane, D. J., Fries, J. F., Cooper, N. S., Healey, L. A., Kaplan, S. R., Liang, M. H., Luthra, H. S., Medsger, T. A., Jr, Mitchell, D. M., Neustadt, D. H., Pinals, R., S., Schiller, J. G., Sharp, J. T., Wilder, R. L. and Hunder, G. G. 1988. The American Rheumatism Association 1987 revised criteria for the classification of rheumatoid arthritis. *Arthritis Rheum.* 31:315.
23 Tan, E. M., Cohen, A. S., Fries, J. F., Masi, A. T., McShane, D. J., Rothfield, N. F., Schaller, J. G., Talal, N. and Winchester, R. J. 1982. The 1982 revised criteria for the classification of systemic lupus erythematosus. *Arthritis Rheum.* 25:1271.
24 Pritchard, J. K. and Przeworsi, M. 2001. Linkage disequilibrium in humans: models and data. *Am. J. Hum. Genet.* 69:1.
25 Glienke, J., Sobanov, Y., Brostjan, C., Steffens, C., Nguyen, C., Lehrach, H., Hofer, E. and Francis, F. 1998. The genomic organization of NKG2C, E, F, and D receptor genes in the human natural killer gene complex. *Immunogenetics* 48:163.
26 Brostjan, C., Sobanov, Y., Glienke, J., Hayer, S., Lehrach, H., Francis, F. and Hofer, E. 2000. The NKG2 natural killer cell receptor family: comparative analysis of promoter sequences. *Genes Immun.* 1:504.
27 Batzer, M. A. and Deininger, P. L. 2002. Alu repeats and human genomic diversity. *Nat. Rev. Genet.* 3:370.
28 Paloneva, J., Kestila, M., Wu, J., Salminen, A., Bohling, T., Ruotsalainen, V., Hakola, P., Bakker, A. B., Phillips, J. H., Pekkarinen, P., Lanier, L. L., Timonen, T. and Peltonen, L. 2000. Loss-of-function mutations in TYROBP (DAP12) result in a presenile dementia with bone cysts. *Nat. Genet.* 25:357.
29 Shum, B. P., Flodin, L. R., Muir, D. G., Rajalingam, R., Khakoo, S. I., Cleland, S., Guethlein, L. A., Uhrberg, M. and Parham, P. 2002. Conservation and variation in human and common chimpanzee CD94 and NKG2 genes. *J. Immunol.* 168:240.
30 Khakoo, S. I., Rajalingam, R., Shum, B. P., Weidenbach, K., Flodin, L., Muir, D. G., Canavez, F., Cooper, S. L., Valiante, N. M., Lanier, L. L. and Parham, P. 2000. Rapid evolution of NK cell receptor systems demonstrated by comparison of chimpanzees and humans. *Immunity* 12:687.
31 Takei, F., McQueen, K. L., Maeda, M., Wilhelm, B. T., Lohwasser, S., Lian, R. H. and Mager, D. 2001. Ly49 and CD94/NKG2: developmentally regulated expression and evolution. *Immunol. Rev.* 181:90.
32 Valiante, N. M., Uhrberg, M., Shilling, H. G., Lienert-Weidenbach, K., Arnett, K. L., D'Andrea, A., Phillips, J. H., Lanier, L. L. and Parham, P. 1997. Functionally and structurally distinct NK cell receptor repertoires in the peripheral blood of two human donors. *Immunity* 7:739.
33 Shilling, H. G., McQueen, K. L., Cheng, N., W., Shizuru, J., A., Negrin, R., S. and Parham, P. 2003. Reconstitution of NK cell receptor repertoire following HLA-matched hematopoietic cell transplantation. *Blood* 101:3730.

BAFF/BLyS can potentiate B-cell selection with the B-cell coreceptor complex

Hidenori Hase, Yumiko Kanno, Masaru Kojima, Kaoru Hasegawa, Daisuke Sakurai, Hidefumi Kojima, Naoyuki Tsuchiya, Katsushi Tokunaga, Nobuhide Masawa, Miyuki Azuma, Ko Okumura, and Tetsuji Kobata

The tumor necrosis factor (TNF)–like ligand BAFF/BLyS (B-cell activating factor of the TNF family/B-lymphocyte stimulator) is a potent B-cell survival factor, yet its functional relationship with other B-cell surface molecules such as CD19 and CD40 is poorly understood. We found that follicular dendritic cells (FDCs) in human lymph nodes expressed BAFF abundantly. BAFF up-regulated a B cell–specific transcription factor Pax5/BSAP (Pax5/B cell–specific activator protein) activity and its target CD19, a major component of the B-cell coreceptor complex, and synergistically enhanced CD19 phosphorylation by B-cell antigen receptor (BCR). BAFF further enhanced B-cell proliferation, immunoglobulin G (IgG) production, and reactivity to CD154 by BCR/CD19 coligation and interleukin-15 (IL-15). Our results suggest that BAFF may play an important role in FDC–B-cell interactions through the B-cell coreceptor complex and a possibly sequential link between the T cell–independent and –dependent B-cell responses in the germinal centers. (Blood. 2004;103:2257-2265)

Introduction

The tumor necrosis factor (TNF) superfamily ligand BAFF (B-cell activating factor of the TNF family), also known as BLyS (B-lymphocyte stimulator), TALL-1 (TNF and apoptosis leukocyte-expressed ligand-1), THANK (TNF homolog that activates apoptosis, nuclear factor–κB, and c-Jun NH2-terminal kinase), and zTNF4, is selectively expressed on macrophages, monocytes, and dendritic cells (DCs) regulated by interferon-γ (IFN-γ).[1] BAFF acts as a potent B-cell growth factor and costimulator of immunoglobulin (Ig) production.[2] BAFF binds to 3 separate receptors, including B-cell maturation antigen (BCMA), transmembrane activator and calcium-modulator and cyclophilin ligand (CAML)–interactor (TACI), and BAFF-R (BAFF receptor). Their expression is restricted mainly to B cells, and BAFF–BAFF-R interactions are required for immature B cells to survive beyond the first transitional stage (T1) in mice.[3] BAFF administration in mice can potentiate antibody (Ab) responses and increase the number of plasma cells.[4,5] In addition, mice transgenic for BAFF showed increased germinal center (GC) formation and developed autoimmune disorders such as production of autoantibodies and Ig deposition in kidney, considered to be symptoms of human systemic lupus erythematosus (SLE).[6] Contrary to this, BAFF-deficient mice have significantly fewer marginal zone and follicular B cells in secondary lymphoid tissue,[7] and TACI-Ig–treated mice lack GCs.[8] Collectively, these finding suggest that BAFF has a crucial role in the control of GC B-cell development and humoral immune responses. However, the cellular and molecular mechanisms of BAFF functions in GCs are still obscure.

In humoral immune responses, follicular dendritic cell (FDC)–B-cell interactions in GCs play a crucial role in full activation of B cells.[9] FDC–B-cell interactions require 2 distinct but synergistic signals. The first signal, delivered through the B-cell antigen receptor (BCR), is provided by antigen (Ag) itself and is responsible for the specificity of the Ab secreted. The second signal is derived from the B-cell coreceptor complex consisting of CD19, CD21 (CR2), and CD81 bound to complement (C) and is not Ag-specific.[10] The B-cell coreceptor complex is essential for the rapid trapping of C-coated Ags by B cells and is critical for early protective Ab responses to lethal pathogens that rapidly multiply and quickly overwhelm the immune system.[11,12] C3 component and its cleavage products such as C3d are particularly important for the efficient opsonization, lysis, and clearance of bacteria.[13] Depletion of C3 in mice reduces T cell–dependent (TD) and some T cell–independent (TI) Ab responses.[14] Similar defects of humoral immune responses are found in patients with genetic deficiencies in C3.[15] In addition, C3-deficient mice have reduced TD and TI antibody responses.[16-19] CD21 is expressed primarily by FDCs and mature B cells, and C3-coated Ags trapped by CD21 on FDCs are also captured by CD21 of the B-cell coreceptor.[11] CD21-deficient mice have impaired humoral immunity due to defective maintenance of B cells within GCs,[20] which is a similar phenotype to that of C3-deficient mice. Thereby, the binding of CD21 with C3-coated Ags in FDC–B-cell interactions may facilitate the processing and presentation of Ags at low concentrations, particularly in the absence of preformed or natural Abs where Fc receptor interactions may also facilitate immune

From the Division of Immunology, Institute for Medical Science, and Department of Pathology, Dokkyo University School of Medicine, Tochigi, Japan; Research Center of Fundamental Medicine, International University of Health and Welfare, Tochigi, Japan; Department of Human Genetics, Graduate School of Medicine, the University of Tokyo, Japan; Department of Molecular Immunology, Tokyo Medical and Dental University, Japan; and Department of Immunology, Juntendo University School of Medicine, Tokyo, Japan.

Submitted August 6, 2003; accepted November 18, 2003. Prepublished online as *Blood* First Edition Paper, November 20, 2003; DOI 10.1182/blood-2003-08-2694.

Supported in part by grants from the NOVARTIS Foundation (Japan) for the Promotion of Science and from the Promotion and Mutual Aid Corporation for Private Schools of Japan.

Reprints: Tetsuji Kobata, Division of Immunology, Institute for Medical Science, Dokkyo University School of Medicine, 880 Kitakobayashi, Mibu, Tochigi 321-0293, Japan; e-mail: tkobata@dokkyomed.ac.jp.

The publication costs of this article were defrayed in part by page charge payment. Therefore, and solely to indicate this fact, this article is hereby marked "advertisement" in accordance with 18 U.S.C. section 1734.

complex processing.[21] Activation of the B-cell coreceptor complex makes B cells more responsive to BCR signals, resulting in positive selection of B cells.[11]

In the B-cell coreceptor complex, CD19 is thought to functionally link CD21 with BCR following corecognition of C3d-coated Ags and is a key player in its activation.[22] CD19 exerts its positive effect on BCR signaling by the phosphorylation-dependent recruitment of Vav and phosphatidylinositol-3 kinase (PI3K), which in turn enhances Ca flux, activation of the extracellular signal-regulated kinase 1/2 (ERK1/2), and ultimately B-cell proliferation.[23-25] CD19 is rapidly phosphorylated on Tyr482 and Tyr513 following BCR ligation.[26-28] Point mutations in CD19, Y482, and Y513 disrupt CD19 function in B-cell differentiation with reduction of splenic germinal centers, B cells, and class switching in vivo.[29] Tyr513 is required for BCR-mediated activation by coupling of PI3K and Src family tyrosine kinases to CD19.[30,31] Expression of CD19 is reported to be under the direct control of the B lineage–specific transcription factor Pax5/B cell–specific activator protein (Pax5/BSAP),[32] which is implicated in isotype switching and cell proliferation of mature B cells in addition to B-cell development.[33] Coligation of CD19 with BCR decreased the signaling threshold for BCR-dependent stimulation and augmented B-cell proliferation.[23]

However, the functional relationship of BAFF with the above B-cell molecules in coordinating B-cell responses in GCs is not fully clear. We show here that FDCs in GCs of human lymph nodes expressed BAFF and that BAFF stimulation synergistically enhanced the BCR signaling by phosphorylation of CD19. In the presence of interleukin-15 (IL-15), BAFF significantly increased B-cell proliferation and IgG production upon BCR and CD19 coligation. These B cells after BCR/CD19 coligation and BAFF stimulation were highly responsive to CD154 (CD40 ligand) stimulation. These findings suggest that BAFF can mediate FDC–B-cell interactions, facilitate B-cell selection through the B-cell coreceptor complex, and subsequently optimize B-cell responses by T-cell help in GCs.

Materials and methods

Cell preparation and cell cultures

Human peripheral blood mononuclear cells were isolated from pooled healthy donors by Ficoll-Hypaque density-gradient centrifugation. After depletion of monocytes by adherence to the plastic surface of culture dishes, E rosette–negative populations were collected with 5% sheep erythrocytes and Ficoll-Hypaque. Purified B cells were isolated by depletion of non-B cells using a B-cell isolation kit and autoMACS (Miltenyi Biotec, Auburn, CA). The resultant B-cell population was less than 2% $CD14^+$, less than 1% $CD3^+$, less than 2% $CD57^+$, and more than 95% $CD20^+$. $CD14^+$ monocytes were recovered from the B cell–depleted fraction. Monocyte-derived dendritic cells corresponding to $CD83^+$ cells were prepared as reported previously.[34] Briefly, monocytes were cultured supplemented with 800 U/mL granulocyte-macrophage colony-stimulating factor (GM-CSF) (PeproTech, Rocky Hill, NJ) and 25 ng/mL IL-4 (PeproTech) for 4 days. The cells were then incubated with GM-CSF and 10 ng/mL TNF-α (PeproTech) for 7 days. Human B-cell lines including Ramos, P32/ISH, Raji, and Daudi cells were purchased from the Human Science Research Resources Bank (Osaka, Japan). Murine fibroblastic L cells expressing human CD32/FcγRII (DT70 cells)[35] were used to coligate BCR and CD19 instead of FDCs. All cultures were conducted in RPMI 1640 medium supplemented with 25 mM HEPES (*N*-2-hydroxyethylpiperazine-*N*′-2-ethanesulfonic acid), 10% fetal calf serum, 2 mM L-glutamine, 1 mM sodium pyruvate, 5.5×10^{-2} mM 2-mercaptoethanol, 100 U/mL penicillin, and 100 U/mL streptomycin (all from Invitrogen, Carlsbad, CA). Mouse B cells were purified from the spleens of 8-week-old C57BL/6 mice (Japan SLC, Shizuoka, Japan) with the use of a mouse B-cell isolation kit and autoMACS (Miltenyi Biotec). The resultant B-cell population was more than 95% $B220^+$.

Antibodies and reagents

The following Abs were used in this study: BAFF (TALL-1) (Santa Cruz Biotechnology, Santa Cruz, CA); phospho-CD19 (Tyr513), CD19 (Cell Signaling Technology, Beverly, MA); IgM, FLAG M2, β-actin (Sigma-Aldrich, St Louis, MO); Igκ, Igλ, fluorescein isothiocyanate (FITC)–labeled CD40, Pax5 (BD PharMingen, San Diego, CA); control mouse IgG1, CD19 (HD37 clone; DAKO, Glostrup, Denmark); FITC-labeled CD14, CD20, HLA-DR, phycoerythrin (PE)–labeled intercellular adhesion molecule-1 (ICAM-1) (CD54) (eBioscience, San Diego, CA); PE-labeled CD19 (Immunotech, Marseille, France); and PE-labeled CD21 (CALTAG, Burlingame, CA). The following reagents were used: IFN-γ (PeproTech), lipopolysaccharide (LPS) (Sigma-Aldrich), *Staphylococcus aureus Cowan I* (SAC) (Calbiochem, La Jolla, CA), recombinant human IL-2 (Invitrogen), recombinant human IL-15 (PeproTech), recombinant human BAFF (PeproTech), and recombinant human TACI-Fc chimera protein (TACI-Ig; Genzyme-Techne, Cambridge, MA) consisting of the extracellular domain of TACI and Fc portion of human IgG1.

Establishment of human BAFF transfectant

To construct a BAFF expression vector, a cDNA encoding full-length human BAFF protein (GenBank no. AF132600), subcloned from peripheral blood mononuclear cells (PBMNCs) using a reverse transcription–polymerase chain reaction (RT-PCR) method with linker primers, was inserted into pBluescript SK(+) (Stratagene, La Jolla, CA) at the *Eco*RI and *Bam*HI sites and finally into the pBCMGS*neo* expression vector[36] at the *Xho*I and *Not*I sites (pBCMGS-BAFF). Murine pre-B cells (cell line 300-19) were electroporated with pBCMGS-BAFF, and stable transfectants were selected by G418 treatment. Cells with high-density BAFF were cloned by fluorescence-activated cell sorter (FACS). The CD154 cDNA-transfected cells and the vector alone–transfected cells (mock) have been described previously.[37] To coculture with B cells, transfectants were treated with mitomycin C (50 μg/mL; Sigma-Aldrich) for 30 minutes at 37°C.

Flow cytometric analysis

After incubation of arbitrary Ab with 2 μg/10^6 cells for 20 minutes on ice, cells were washed and resuspended in propidium iodide solution and analyzed using FACSCalibur and associated CellQuest software (both from Becton Dickinson, San Jose, CA). In some experiments, FITC-labeled rabbit antibody to mouse IgG1 (ICN/CAPPEL, Aurora, OH) or FITC-labeled swine antibody to goat IgG (CALTAG) was used as a second Ab. Isotype-matched mouse IgG control was used throughout the studies and always reacted with less than 5% of the cells.

Generation of antihuman BAFF monoclonal antibody

A BALB/c mouse was immunized with human BAFF-expressing transfectant cells 3 times at 10-day intervals. Three days after the final immunization, the splenocytes were fused with NS-1 cells (purchased from Human Science Research Resources Bank), and HAT (hypoxanthine aminopterin thymidine) selection and cloning of hybridomas were performed simultaneously using a hybridoma cloning kit (ClonaCell-HY; StemCell Technologies, Vancouver, BC). Antihuman BAFF designated 1D6 (mouse IgG1, κ) was established and purified from ascitic fluid by using MAbTrap Kit (Amersham Biosciences, Piscataway, NJ).

Immunohistochemical analysis

Biopsied human lymph nodes were fixed in buffered formalin, routinely processed, and embedded in paraffin. After preparation of serial sections, deparaffinization and microwave antigen retrieval using citrate buffer (pH 6.0) were performed. For immunohistochemistry, the sections were stained by the streptavidin-biotin-peroxidase method (Immunotech) using 1D6

monoclonal antibody (mAb), anti-CD21 mAb (2G9; Novocastra, Newcastle, United Kingdom), and anti-FDC mAb (CNA.42; DAKO), accordingly to the instructions provided by the manufacturer. The sections treated with normal mouse serum served as negative controls.

Immunoblot analysis

Phosphate-buffered saline (PBS)–washed cell pellets were resuspended with 0.5% sodium dodecyl sulfate (SDS) solution and boiled for 5 minutes. Proteins (5 to 8 μg) were separated by SDS-polyacrylamide gel electrophoresis (SDS-PAGE), transferred to an Immobilon-P membrane (Millipore, Billerica, MA), blocked with 5% skim milk, and immunoblotted with arbitrary Ab and horseradish peroxidase (HRP)–labeled secondary Ab. Blotting was developed by using the enhanced chemiluminescent substrate (SuperSignal West Pico; Pierce Chemical, Rockford, IL) and visualized with a LumiVision analyzer (Taitec, Tokyo, Japan). The densitometric analysis was performed by using a LumiVision analyzer (Taitec).

Electrophoretic mobility shift assay (EMSA)

We carried out electrophoretic mobility shift assay (EMSA) with Pax5 gel shift oligonucleotides (Santa Cruz) and mutant oligonucleotides (Santa Cruz). These oligonucleotides were 3′ end-labeled with digoxigenin (DIG) by the DIG Oligonucleotide 3′-end Labeling kit (Roche Diagnostics, Penzberg, Germany). Next, 2.5 ng labeled oligonucleotide was incubated at room temperature for 20 minutes with 1 μg poly–deoxy-inosinic-deoxycytidylic acid (dIdC) (Roche Diagnostics) and 5 μg nuclear extracts that were isolated by nuclear extract kit (Active Motif, Carlsbad, CA) in a total volume of 20 μL. DNA probe and protein complexes were resolved by electrophoresis through 5% polyacrylamide gel at 150 V for 45 minutes in 0.5 × Tris–borate–ethylenediaminetetraacetic acid (TBE). To determine the specificity of Pax5 binding activity, a 50-fold excess of unlabeled Pax5 probe was added. For supershift experiments, nuclear extracts were incubated with 2 μL anti-Pax5 antibody for 30 minutes. DNA probes were blotted onto a Hybond-N+ (Amersham Biosciences) and detected using DIG Luminescent Detection kit (Roche Diagnostics) and an ECL-Mini Camera (Amersham Biosciences).

Construction of 3 × FLAG-sBAFF fusion protein

A short version of soluble BAFF (sBAFF/short, amino acid [aa] Gln136-Leu285)[38] was amplified using PCR. sBAFFs were resubcloned as *Hind*III-*Bam*HI fragments into the 3 × FLAG-CMV-9 vector (Sigma-Aldrich). After transfection of the 3 × FLAG-sBAFF vector into COS-7 with cationic liposome reagent (Lipofectamine reagent; Invitrogen), supernatants were collected. Binding of 3 × FLAG-sBAFF to B cells was evaluated by FACS analysis using anti-FLAG M2 mAb (IgG1) and FITC-labeled antimouse IgG1 Ab.

Real-time PCR

Each cDNA sample was analyzed in duplicate by a method for real-time quantitative RT-PCR using the GeneAmp 5700 sequence detection system (Applied Biosystems, Foster City, CA). Quantitative assessment of DNA amplification was detected through the dye SYBR Green according to the manuals provided by the manufacturer for SYBR Green PCR Master Mix (Applied Biosystems). The thermal cycling conditions were 50°C for 2 minutes and 95°C for 10 minutes, followed by 40 cycles of amplification at 95°C for 15 seconds and 60°C for 1 minute for denaturing, annealing-extension, respectively. The following sense and antisense primers were used. TACI: 5′-CAATGTGCATACTTCTGTGAGA-3′ and 5′-AACTTCTCCACTCCGCTGTCTCCTGA-3′; BCMA: 5′-CAACCATTCTTGTCACCACGAA-3′ and 5′-TCTATCTCCGTAGCACTCAAAGCA-3′; BAFF-R: 5′-CAAGGTCATCATTCTGTCTCCG-3′ and 5′-CGGCTCCCTGCTATTGTTGCTCA-3′; and β-actin: 5′-TCACCCACACTGTGCCCATCTACGA-3′ and 5′-CAGCGGAACCGCTCATTGCCAATGG-3′.

Proliferation assay

Purified B cells from human peripheral blood were cultured in a 96-well plate (1×10^5 per well) with mitomycin-treated transfectants expressing BAFF or CD154 (2×10^4 per well) in the presence or absence of SAC and IL-2 (50 U/mL). For coligation experiments, B cells pretreated with anti-BCR mAbs (anti-Igκ and anti-Igλ, 1 μg/mL) and/or anti-CD19 mAb (0.5 μg/mL) were cultured with or without sBAFF (0.1 μg/mL) in a 96-well plate (1×10^5 per well) precoated with mitomycin-treated DT70 cells (2×10^4 per well) in the presence or absence of IL-15 (50 ng/mL). In some experiments, mitomycin-treated CD154 transfectant was also added to the culture (1×10^4 per well). B-cell proliferation was quantitated by pulsing the cells during the last 18 hours of a total of 72 hours of culture with 0.5 μCi (18.5 kBq) per well of [^{3}H]thymidine (Amersham Biosciences).

Detection and quantification of in vitro IgG secretion

Human peripheral blood B cells pretreated with anti-BCR mAbs (anti-Igκ and anti-Igλ, 1 μg/mL) and/or anti-CD19 mAb (0.5 μg/mL) were cultured with or without sBAFF (0.1 μg/mL) in a 96-well plate (1×10^5 per well) precoated with mitomycin-treated DT70 cells (2×10^4 per well) in the presence or absence of IL-15 (50 ng/mL). In some experiments, mitomycin-treated CD154 transfectant was also added to the culture (1×10^4 per well). IgG levels in the supernatants after 10 days of culture were determined by enzyme-linked immunosorbent assay (ELISA) using antihuman Ig (Southern Biotechnology, Birmingham, AL) as the capture Ab and HRP-labeled goat antihuman IgG (Southern Biotechnology) as the detector Ab. After addition of p-nitrophenyl phosphate substrate (Sigma-Aldrich), the amount of IgG present was assessed by spectrophotometric analysis at 490 nm using a model 550 Microplate Reader (Bio-Rad Laboratories, Hercules, CA).

Statistical analysis

All data were expressed as mean ± SD. Differences between groups were examined for statistical significance using the Student *t* test. A *P* value less than .05 denoted the presence of a statistically significant difference.

Results

Establishment of antihuman BAFF mAb and its identification of FDCs in GCs

To evaluate the role of BAFF in human B-cell responses, we developed an antihuman BAFF mAb. For this purpose, we first established a transfectant stably expressing human BAFF on the cell surface and analyzed the B-cell costimulatory activity. BAFF cDNA was cloned into a mammalian expression vector pBCMGS-*neo* from RNA of peripheral blood mononuclear cells by RT-PCR and transfected into murine pre–B-cell line 300-19 cells. Stable expression of human BAFF on the cDNA transfectant but not on mock-transfected cells was verified by functional and immunoblot analyses (Figures 1 and 2A-B). Peripheral blood B cells were cultured with mitomycin-treated transfectants in the presence of suboptimal doses of SAC and IL-2 for BCR stimulation and activation. Flow cytometric analysis showed that addition of BAFF cDNA-transfected cells or CD154 transfectant clearly up-regulated cell surface expression of CD40, ICAM-1, and HLA-DR on B cells compared with that by mock transfectant (Figure 1A). Consistent with the previous report,[38] the level of [^{3}H]thymidine incorporation of B cells induced by BAFF cDNA-transfected cells was increased in a dose-dependent manner with levels comparable to those by CD154 transfectants while mock transfectant showed almost the basal level (Figure 1B). Immunoblot analysis using commercially available polyclonal antihuman BAFF Ab revealed that BAFF cDNA-transfected cells expressed the BAFF molecule. These results indicate that BAFF cDNA-transfected cells expressed functional BAFF molecules on the cell surface, which could deliver

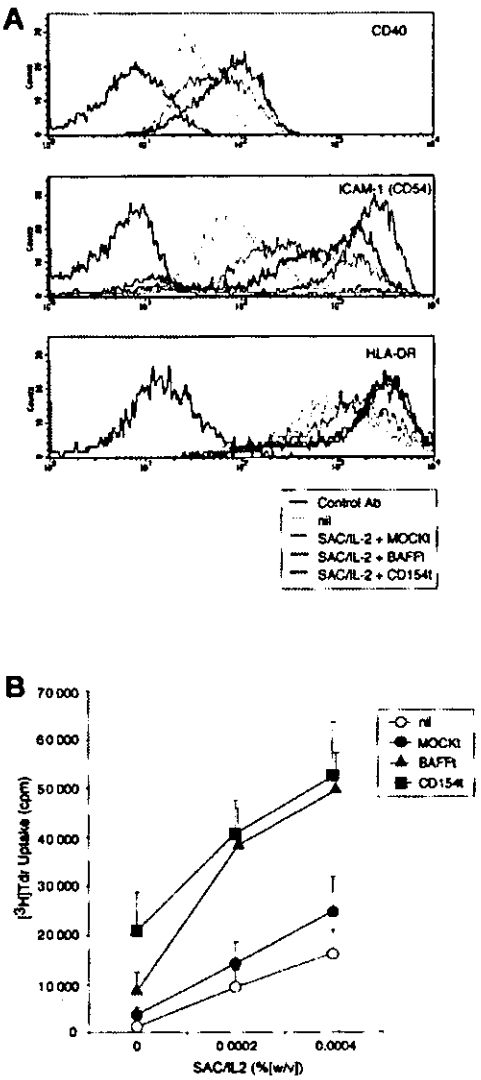

Figure 1. Functional characterization of BAFF transfectant. (A) Human peripheral blood B cells (1×10^5 per well) were cultured with or without mitomycin-treated transfected cells (2×10^4 per well) in the presence or absence of SAC (0.0002% [wt/vol]) and IL-2 (50 U/mL). After treatment for 48 hours, the expression level of CD40, ICAM-1, and HLA-DR was analyzed by FACS analysis. (B) B cells (1×10^5 per well) were cocultured in triplicate in 96-well plates with mitomycin-treated transfected cells (2×10^4 per well) in the presence or absence of SAC (0.0002% [wt/vol] or 0.0004% [wt/vol]) and IL-2 (50 U/mL), and [^{3}H]thymidine (0.5 μCi [18.5 kBq] per well). Incorporation of B cells was measured during the last 18 hours of a total of 72 hours. Data are mean ± SD of triplicate wells and are representative of 3 different experiments.

a B-cell costimulatory signal. This BAFF transfectant was used for further experiments (Figures 3,5). We then immunized a BALB/c mouse with BAFF transfectant and fused the splenocytes with NS-1 myeloma cells. The hybridomas producing antihuman BAFF mAb were screened by specific reactivity to BAFF transfectant. As shown in Figure 2A-B, one mAb, designated 1D6, was obtained, which bound to BAFF transfectant but not to mock transfectant. 1D6 mAb reacted with activated monocytes exposed to IFN-γ, and its expression was further enhanced by the additional treatment with LPS (Figure 2C). As reported previously,[39] monocyte-derived DCs also expressed BAFF (data not shown). Interestingly, we found that 1D6-positive cells were mainly localized in GCs of human lymph nodes where the cells with long processes formed a reticular meshwork (Figure 2D). Immunohistochemical analysis using serial tissue sections revealed that the cells stained with 1D6 mAb were also stained with anti-FDC mAb (Figure 2D) and anti-CD21 mAb (data not shown), suggesting that they were FDCs.

Up-regulation of Pax5/BSAP and CD19 by BAFF

The above finding that FDCs in GCs expressed abundant BAFF raised the possibility that BAFF mediates FDC–B-cell interactions in GCs. To test this notion, we examined the effect of BAFF on the expression of CD19 and CD21 on peripheral blood B cells. CD19 and CD21 together compose the B-cell coreceptor complex that plays a crucial role in B-cell responses of FDC–B-cell interactions.[10] As shown in Figure 3A, BAFF transfectant exhibited a slight but definite up-regulation of CD19 and CD20 expression, but not CD21 expression, on B cells compared with mock transfectant. Because the expression levels of CD19 and CD20 are directly regulated by a B cell–specific transcription factor Pax5/BSAP,[33,40] we next examined the effect of BAFF on Pax5 expression and its DNA binding activity by immunoblot analysis and EMSA. As shown in Figure 3B-C, consistent with up-regulated CD19 and CD20 expression by BAFF transfectant, BAFF transfectant as well as CD154 transfectant clearly increased Pax5 expression and its DNA binding activity in B cells. These results suggest that BAFF induced Pax5 activation and subsequently CD19 and CD20 up-regulation.

Synergistic effect of BAFF on CD19 phosphorylation by BCR

To further confirm the functional relationship between BAFF and the B-cell coreceptor complex, we next examined the effect of BAFF on phosphorylation of CD19 induced by BCR ligation. BCR signaling is known to phosphorylate CD19 on Tyr513, resulting in lowering of the signaling thresholds for B-cell activation, which in turn amplifies BCR signaling.[31] No CD19 phosphorylation was detected in human peripheral blood B cells after BCR ligation (data not shown), probably due to the relatively lower expression of BCR, CD19, and receptors for BAFF (Figure 4). We then estimated the expression of these molecules in various human B-cell lines by flow cytometric and real-time RT-PCR analyses. For this purpose, we prepared recombinant soluble BAFF, which contains the receptor binding domain and an N-terminal FLAG tag, and screened for B-cell lines with high affinity to this recombinant soluble BAFF. As shown in Figure 4A, Ramos, P32/ISH, and Raji, but not Daudi, cell lines exhibited a high affinity to soluble BAFF. In accordance with this, the transcription level of 3 receptors for BAFF, including TACI, BCMA and BAFF-R, revealed high expression in these 3 cell lines (Figure 4B). Among these 3 cell lines, Ramos and P32/ISH cell lines showed the strongest expression of BCR and CD19 (Figure 4A). We then evaluated the effect of BAFF on CD19 phosphorylation on Tyr513 following BCR ligation. As shown in Figure 5, BAFF as well as CD154 stimulation synergistically enhanced the phosphorylation level of CD19 in Ramos cells ($P < .01$) and modestly did so in P32/ISH cells ($P < .05$) after BCR ligation, which was significantly suppressed by TACI-Fc chimera protein (TACI-Ig). Because 1D6 mAb cannot block the binding of BAFF with its receptors, we used TACI-Ig for blocking experiments. On the other hand, Raji cells failed to induce obvious phosphorylation of CD19 (data not shown), which was reflected by the low level of surface BCR compared with other cell lines (Figure 4A). Daudi cells showed no difference in CD19 phosphorylation level with or without BAFF stimulation (data not shown), probably due to undetectable expression of receptors for BAFF (Figure 4). In addition, we examined the effect of BAFF on

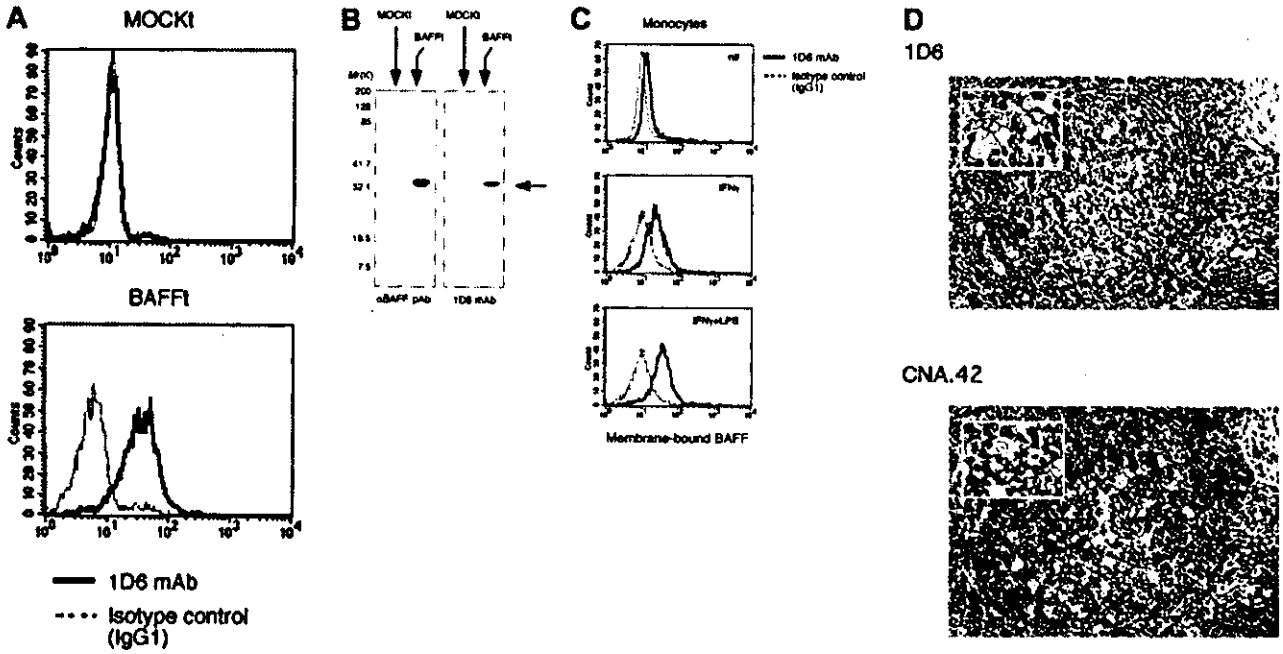

Figure 2. Characterization of 1D6 mAb and identification of BAFF-positive cells within GCs. (A) FACS analysis of BAFF expression using 1D6 mAb. BAFF transfectants and mock transfectants were stained with 1D6 mAb (solid lines) or isotype-matched control Ab (IgG1) (dashed lines) followed by FITC-conjugated Ab to mouse IgG1. (B) Cell lysates were prepared from BAFF transfectants and mock transfectants and subjected to immunoblotting analysis using 1D6 mAb or antihuman BAFF (TALL-1) polyclonal Ab. (C) Peripheral blood monocytes ($CD14^+$ cells more than 98%) were activated by IFN-γ (1000 U/mL) and LPS (10 ng/mL) for 24 hours. After blocking with normal mouse serum plus control IgG1 mouse mAb, BAFF expression was evaluated by FACS analysis using 1D6 mAb. (D) BAFF-positive cells or FDCs (brown) localized in GCs, as determined by immunohistochemical staining of serial human lymph node sections with 1D6 mAb or CNA.42 mAb, respectively (magnification × 200). (Inset) High magnification (× 400). Nuclei were visualized by hematoxylin staining. Data shown are representative of 3 different experiments.

CD19 phosphorylation in murine splenic B cells after BCR ligation because it has been reported that BCR-mediated CD19 phosphorylation is well established in murine B cells[31] and that human BAFF is active on mouse B cells.[1] BAFF stimulation synergistically enhanced BCR-mediated CD19 phosphorylation in murine splenic B cells ($P < .01$), which was significantly suppressed by TACI-Ig. Taken together, these results indicated that BAFF synergistically amplified CD19 phosphorylation induced by BCR ligation, which is relevant to enhanced B-cell activation mediated by the B-cell coreceptor complex.

B-cell responses induced by BAFF with the B-cell coreceptor complex

The above findings encouraged us to examine the role of BAFF in B-cell responses mediated by the B-cell coreceptor complex in FDC–B-cell interactions. For this purpose, we measured the effect of BAFF on human peripheral blood B-cell proliferation and in vitro IgG production under the conditions of coligation of BCR with CD19 in the presence of IL-15. To mimic FDC–B-cell interactions through the coengagement of BCR and CD19/CD21 with C3-coated Ags, we used murine fibroblastic L cells expressing CD32/FcγRII to cross-link anti-BCR and anti-CD19 mAbs bound to B cells instead of FDCs and used soluble recombinant BAFF instead of BAFF transfectant for increasing cell-cell contacts between peripheral blood B cells and L cells. IL-15 is produced by various Ag-presenting cells and is indispensable for the DC-induced IgG secretion in vitro.[39] Under these conditions, BAFF clearly up-regulated CD40 expression on B cells in the presence of BCR/CD19 coligation, which was completely inhibited by TACI-Ig, although BCR/CD19 coligation itself showed less up-regulation of CD40 (Figure 6A). Coligation of BCR/CD19 resulted in an increase of $[^3H]$thymidine incorporation in B cells compared with that induced by anti-BCR or anti-CD19 mAb alone, as reported previously.[23] Importantly, BAFF further enhanced B-cell proliferation induced by coligation of BCR/CD19 ($P < .05$), which was completely inhibited by TACI-Ig (Figure 6B). Consistent with B-cell proliferation, BAFF further enhanced B-cell IgG production in the presence of BCR/CD19 coligation ($P < .01$), which was also completely inhibited by TACI-Ig (Figure 6C). These results clearly indicated that BAFF can facilitate B-cell responses mediated by the B-cell coreceptor complex, suggesting that BAFF can facilitate B-cell selection by FDCs in GCs.

Finally, to examine the effect of BAFF on B-cell responses to CD154 after BCR/CD19 coligation, we added the CD154 transfectant to the above culture conditions because results shown in Figure 1A and Figure 6A clearly showed up-regulation of CD40 expression on B cells in response to BAFF. As expected, the CD154 transfectant additively enhanced B-cell proliferation and IgG production induced by BAFF in the presence of BCR/CD19 coligation ($P < .05$) (Figure 6B-C). These results suggest that BAFF can help the same B cells to prepare for sequential TD B-cell responses after FDC–B-cell interactions.

Discussion

The B-cell zone of primary and secondary follicles contains a network of FDCs. FDCs appear to be specialized to capture Ags in the form of opsonized Ags, such as immune complexes consisting of Ag, Ab, and C, by receptors for Fc and C. Ags are not internalized but remain intact on the FDC surface, where they can be recognized by B cells. Thus, FDCs are potent accessory cells for B cells in GCs, but the molecular basis of their activity is not understood. Several important molecules involved in FDC–B-cell

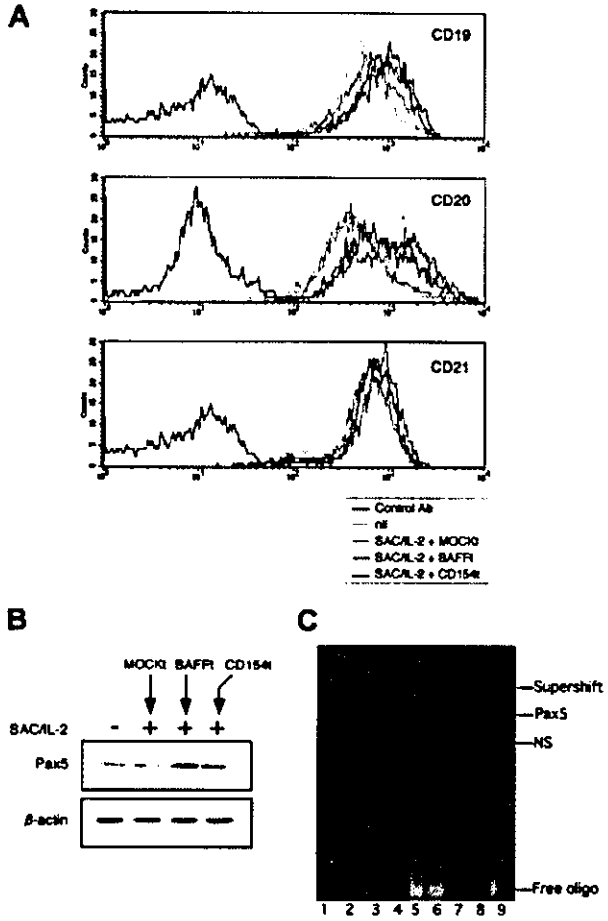

Figure 3. Up-regulation of Pax5/BSAP and CD19 by BAFF. Human peripheral blood B cells were cultured with or without mitomycin-treated transfectants at a ratio of 10:2 in the presence or absence of SAC (0.0002% [wt/vol]) and IL-2 (50 U/mL). (A) After the treatment for 48 hours, the expression level of CD19, CD20, and CD21 was evaluated by FACS analysis. After treatment for 48 hours in the above conditions (A), cell lysates and nuclear extracts were prepared for immunoblot analysis using anti-Pax5 Ab (B) and EMSA using oligonucleotides containing Pax5 binding site (C), respectively. Lane 1, Pax5 oligonucleotide alone; lane 2, Pax5 mutant oligonucleotide alone; lane 3, B cell alone plus Pax5 oligonucleotides; lane 4, SAC/IL-2–stimulated B cells plus mock transfectants plus Pax5 oligonucleotides; lane 5, SAC/IL-2–stimulated B cells plus CD154 transfectants plus Pax5 oligonucleotides; lane 6, SAC/IL-2–stimulated B cells plus BAFF transfectants plus Pax5 oligonucleotides; lane 7, SAC/IL-2–stimulated B cells plus BAFF transfectants plus Pax5 mutant oligonucleotides; lane 8, SAC/IL-2–stimulated B cells plus BAFF transfectants plus Pax5 oligonucleotides plus competitor; lane 9, SAC/IL-2–stimulated B cells plus BAFF transfectants plus Pax5 oligonucleotides plus anti-Pax5 Ab. NS indicates nonspecific band. Data shown are representative of 3 different experiments.

interactions have been identified by blocking the ligands and receptors on FDCs and/or B cells.[9] For example, the engagement of CD21 of the B-cell coreceptor complex by C-coated Ags on FDCs delivers a crucial signal through CD19 that markedly augments the stimulation delivered by the binding of Ags to the BCR. Thus, the B-cell coreceptor complex plays a pivotal role in B-cell selection, in which only B cells with higher affinity can be positively selected even in low concentrations of Ags and rewarded with a survival signal. The B-cell receptor complex thus promotes B-cell responses. During their passage through GCs, mature B cells undergo apoptosis if they encounter self-Ags or if they are not positively selected by an antigenic signal.

In this study, we provide several evidences for a new role of BAFF in B-cell responses in GCs through FDC–B-cell interactions. First, we developed a novel antihuman BAFF mAb (1D6). Immunohistochemical analysis using 1D6 mAb demonstrated that

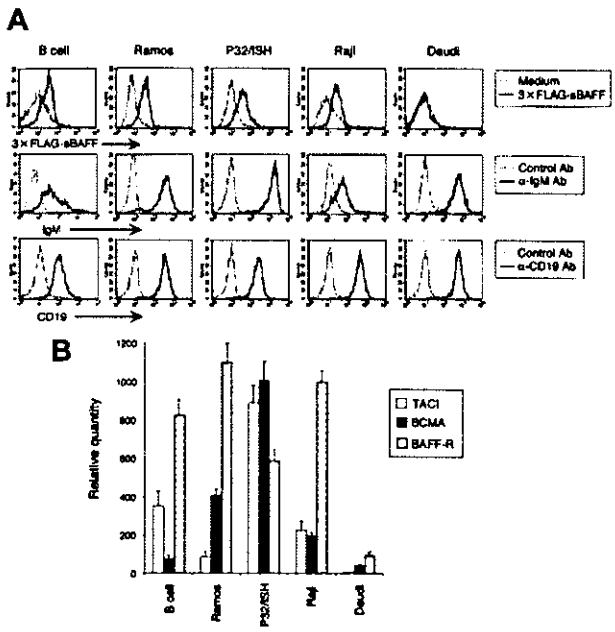

Figure 4. BAFF receptor expression in human B cells. (A) Cells were stained with 3 × FLAG-sBAFF supernatant followed by anti-FLAG M2 mAb with FITC-labeled antimouse IgG1 Ab, or anti-IgM Ab followed by FITC-labeled antigoat Ab, or directly PE-labeled anti-CD19 mAb. Expression was analyzed by FACS. (B) The expression of BAFF receptors was evaluated by real-time quantitative RT-PCR for TACI, BCMA, and BAFF-R, as described in Figure 3B. The amount of transcription was normalized to the level of β-actin and designated as a relative quantity. Data shown are representative of 3 different experiments.

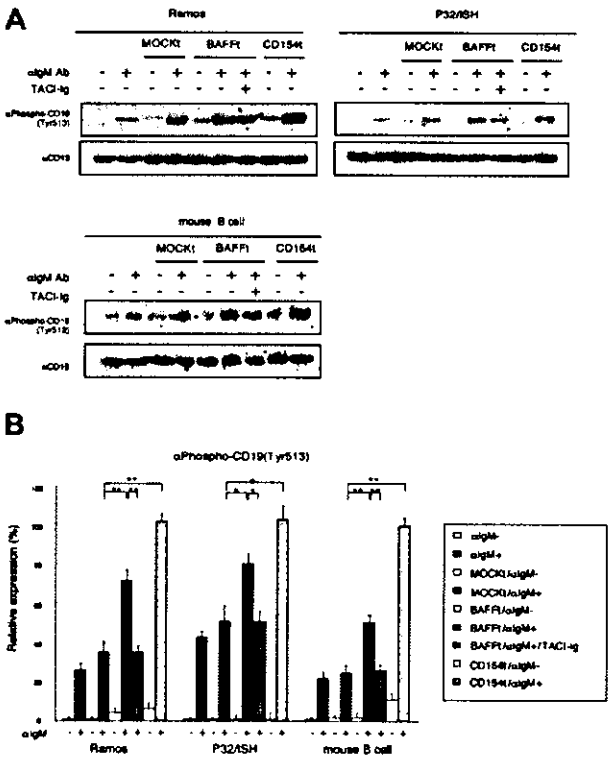

Figure 5. Synergistic effect of BAFF CD19 phosphorylation by BCR. (A) After coculture of human B-cell lines or murine splenic B cells with mitomycin-treated transfectants at a ratio of 10:2 for 3 hours, BCR ligation was induced by antihuman or antimouse IgM Ab (0.5 μg/mL). After 5 minutes, the reaction was terminated and cell lysates were prepared for immunoblot analysis using antiphospho CD19 (Tyr513) Ab. The expression levels of phophorylated CD19 are presented in the histogram in panel B. CD19 was detected as a loading control. For the blocking assay, TACI-Ig fusion protein was used at 0.4 μg/mL. Data shown are representative of 3 different experiments and are presented as mean ± SD; $^{*}P < .05$; $^{**}P < .01$.

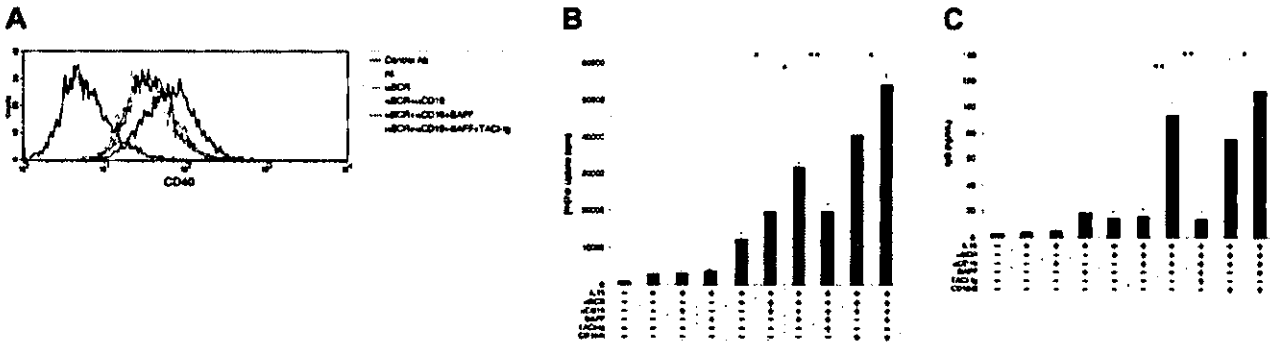

Figure 6. Effects of BAFF on B-cell responses with coligation of BCR and CD19. Human peripheral blood B cells (1×10^5) pretreated with anti-BCR mAbs (anti-Igκ and anti-Igλ; 1 μg/mL), anti-CD19 mAb (0.5 μg/mL), and/or control mAb (1 μg/mL) were cultured with or without sBAFF (0.1 μg/mL) in triplicate in 96-well plates precoated with mitomycin-treated DT70 cells (2×10^4 per well) in the presence or absence of IL-15 (50 ng/mL) together with or without mitomycin-treated CD154 transfectant (1×10^4 per well). (A) After treatment for 48 hours, the expression level of CD40 was analyzed by FACS analysis. (B) [^{3}H]thymidine (0.5 μCi [18.5 kBq] per well) incorporation of B cells was measured during the last 18 hours of a total of 72 hours. (C) After 10 days, IgG concentration in the supernatant was measured by ELISA. For the blocking assay, TACI-Ig fusion protein was used at 0.4 μg/mL. The values are reported as the mean ± SD of triplicate wells, and data shown are representative of 3 different experiments; $^*P < .05$; $^{**}P < .01$.

FDCs in GCs of human lymph nodes expressed BAFF abundantly (Figure 2). To date, although it has been reported that BAFF is produced by macrophages, monocytes, DCs, and activated neutrophils,[2,41] the present study is the first to demonstrate that FDCs in GCs of human lymph nodes express BAFF. This finding prompted us to perform further experiments.

We next showed that BAFF stimulation enhanced the expression of a B cell–specific transcription factor, Pax5/BSAP, and its target molecule CD19 (Figure 3). Our finding about Pax5 expression and its DNA binding activity was in agreement with that reported by other investigators, who reported increased levels of Pax5 following CD154 stimulation.[42] The conditional inactivation of Pax5 in late B lymphopoiesis led to a preferential loss of mature B cells in peripheral lymphoid organs and to the absence of recirculating B cells in the bone marrow,[43] and this phenotype closely resembles that of BAFF-deficient mice.[7]

We found that BAFF simulation significantly increased the ability of BCR to phosphorylate CD19 (Figure 5). CD19 is tyrosine phosphorylated when BCR is ligated, and the basis for phosphorylation is the association of CD19 with tyrosine kinases (Lyn and Syk) and other components of the BCR complex consisting of CD22, Ig-α, and Ig-β.[44] The tyrosine phosphorylation of CD19 at Tyr513 is required for amplifying BCR-mediated activation by coupling of PI3K, and BLNK links BCR-activated Syk kinase to phosphorylated CD19 Y513 to enhance the BCR signaling. We observed that the magnified capacity of BCR to phosphorylate CD19 after BAFF stimulation was more prominent in Ramos cells than in P32/ISH cells (Figure 5A). A probable explanation for this was presented by a recent study showing that TACI is a negatively regulatory receptor for BAFF signaling.[45] Ramos cells displayed barely detectable TACI expression while P32/ISH expressed a relatively high level (Figure 4B), suggesting that TACI signaling might have a suppressive effect on phosphorylation of CD19. At present, the precise molecular mechanisms by which BAFF synergistically augments CD19 phosphorylation by BCR ligation are unknown. However, it is possible that BAFF signaling was integrated at the Lyn/Syk activation pathway, distinct from a signal for the Pax5 activation pathway leading to CD19 and BLNK up-regulation.[46] It has been reported that CD40 engagement resulted in increased phosphorylation of Lyn in B cells.[47] Alternatively, BAFF might inhibit phosphatase SHP1 activity, which suppresses Syk.[44]

Finally, we demonstrated that when CD19 was coligated directly with BCR in the presence of IL-15, which mimics FDC–B-cell interactions, BAFF stimulation further enhanced B-cell proliferation and caused secretion of IgG (Figure 6B-C). Thus, BAFF can be involved in FDC–B-cell interactions in GCs to potentiate the primary response of B cells to Ags in concert with the B-cell coreceptor complex. Detectable levels of IgG production were not observed in the presence of BCR/CD19 coligation without BAFF stimulation (Figure 6C). Thus, it is possible that BAFF is required for plasma cell differentiation and IgG production in TI immune responses through FDC–B-cell interactions, because B cells proliferated in the same conditions. Furthermore, we demonstrated that after FDC–B-cell interaction induced by BAFF, B cells up-regulated CD40 expression and became susceptible to CD154, which is expressed on activated T cells. Notably, coligation of BCR/CD19 without BAFF failed to up-regulate CD40 (Figure 6A), in which substantial B-cell proliferation was observed. Taken together, these findings suggest that BAFF can play a crucial role in TI B-cell responses in FDC–B-cell interactions through the B-cell coreceptor complex and can transfer its B-cell specificity to TD immune responses (Figure 7). A small number of $CD4^+$ T cells are reported to be present in GCs, so-called GC T cells or follicular B-helper T cells, which express CD154.[48] Thus, CD40 engagement by GC T cells may elicit optimal B-cell responses after or simultaneously with FDC–B-cell interactions by BAFF. In addition, enhanced HLA-DR and ICAM-1 expression by BAFF (Figure 1A) would contribute to enhanced Ag presentation and adhesion to T cells. Consistent with this, the TD but not TI IgG

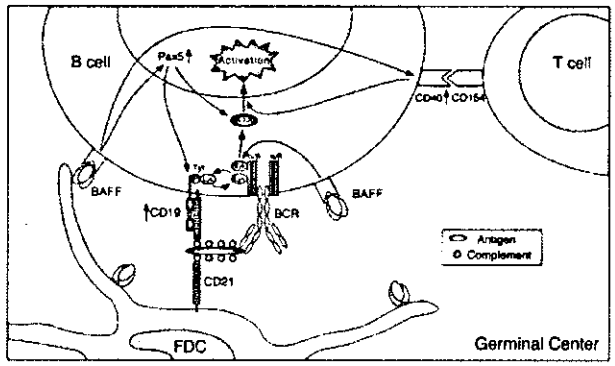

Figure 7. Proposed scheme of B-cell activation with BAFF in GCs. GC B cells receive signals for activation by FDCs through the BCR and B-cell coreceptor complex. The B-cell responses are further enhanced by BAFF providing CD19 and probable BLNK up-regulation through Pax5 activation and the high ability of BCR to phosphorylate CD19, which in turn amplifies BCR signaling. Moreover, up-regulation of CD40 by BAFF renders the same B cells more susceptible to T-cell help by CD154. See "Discussion" for details.

response is impaired in CD154-deficient mice,[49,50] whereas BAFF deficiency impairs both TD and TI IgG production,[7] suggesting that BAFF sequentially links TI and TD B-cell responses.

Interestingly, the transcript for activation-induced cytidine deaminase (AID), which plays a critical role in both Ig somatic hypermutation and class switching in B cells,[51] was found to be up-regulated by BAFF stimulation in addition to CD154 stimulation (Litinskiy et al[39] and H. H. et al, unpublished data, December 2002). Thus, in addition to TI Ig class switching,[39] it is likely that BAFF also produces high-affinity B-cell mutants, suggesting that BAFF is involved in affinity maturation of B cells even under TI conditions.

GCs are the primary sites for affinity maturation coupled with Ag-driven clonal selection (selection of B-cell mutants) and development of B-cell memory and plasma cells. The survival of B-cell mutants in GCs is dependent on their ability to compete for Ag on the surface of FDCs. Only high-affinity mutants are able to compete and retrieve Ags from FDCs and interact with GC helper T cells. In contrast, GC B cells with lower-affinity BCR fail to compete for Ags on FDCs and are consequently eliminated by apoptosis. Thus, the ability of the B-cell coreceptor complex to decrease the signaling thresholds for BCR stimulation in FDC–B-cell interactions plays a quite important role in B-cell selection. The development of SLE in humans is associated with abnormalities of B-cell functions, and an altered expression pattern of CD21 on B cells has been reported.[52] Failure of CD21 expression was also found in a human SLE model mouse, MRL/lpr.[53] Overexpression of CD19 is associated with autoimmunity in mice,[54] and abnormalities in CD19 expression are observed in the human autoimmune disease scleroderma.[55] The binding of C-coated self-Ags to CD21, despite low-affinity BCRs, may promote clonal expansion of self-reactive B cells and be involved in the selection of the repertoire of natural antibodies, suggesting a defect in peripheral tolerance of B cells in FDC–B-cell interactions in GCs, where BAFF can further help self-reactive B cells to escape from apoptosis. Indeed, BAFF overexpression increased IgG, IgA, and IgE production and led to an SLE-like syndrome with kidney deposition of IgG and IgA.[6,56] Thus, it is most likely that BAFF regulates peripheral tolerance through the B-cell coreceptor complex. This new role for BAFF in FDC–B-cell interactions in concert with the B-cell coreceptor complex suggests that BAFF-induced accumulation of self-reactive B cells might be the result of direct effects on their survival and selection rather than simple expansion of the B-cell compartment, thereby increasing the number of responders. BAFF may therefore play an important role in regulating immunity and tolerance by controlling the development of B cells.

Acknowledgments

We thank Dr Hajime Karasuyama for the pBCMGS*neo* expression vector, Dr Akira Niwa for helpful discussion, and Ms Yoshie Nitta for excellent secretarial assistance. We also thank the Laboratory Animal Research Center and Laboratory of Analytical Instruments, Institute for Medical Science, Dokkyo University School of Medicine, for the use of their facilities and thank the Japanese Red Cross Tochigi Blood Center for leukopaks. We also thank Dr F. G. Issa for critical reading of the manuscript.

References

1. Moore PA, Belvedere O, Orr A, et al. BLyS: member of the tumor necrosis factor family and B lymphocyte stimulator. Science. 1999;285:260-263.
2. Mackay F, Browning JL. BAFF: a fundamental survival factor for B cells. Nat Rev Immunol. 2002;2:465-475.
3. Tompson JS, Bixler SA, Qian F, et al. BAFF-R, a newly identified TNF receptor that specifically interacts with BAFF. Science. 2001;293:2108-2111.
4. Karpusas M, Cachero TG, Qian F, et al. Crystal structure of extracellular human BAFF, a TNF family member that stimulates B lymphocytes. J Mol Biol. 2002;315:1145-1154.
5. Do RKG, Hatada E, Lee H, Tourigny MR, Hilbert D, Chen-Kiang S. Attenuation of apoptosis underlies B-lymphocyte stimulator enhancement of humoral immune response. J Exp Med. 2000;192:953-964.
6. Mackay F, Woodcock SA, Lawton P, et al. Mice transgenic for BAFF develop lymphocytic disorders along with autoimmune manifestations. J Exp Med. 1999;190:1697-1710.
7. Schiemann B, Gommerman JL, Vora K, et al. An essential role for BAFF in the normal development of B cells through a BCMA-independent pathway. Science. 2001;293:2111-2114.
8. Yan M, Marsters SA, Grewal IS, Wang H, Ashkenazi A, Dixit VM. Identification of a receptor for BLyS demonstrates a crucial role in humoral immunity. Nat Immunol. 2000;1:37-41.
9. Tew JG, Wu J, Fakher M, Szakal AK, Qin D. Follicular dendritic cells: beyond the necessity of T-cell help. Trends Immunol. 2001;22:361-367.
10. Fearon DT, Carter RH. The CD19/CR2/TAPA-1 complex of B lymphocytes linking natural to acquired immunity. Annu Rev Immunol. 1995;13:127-149.
11. Poe JC, Hasegawa M, Tedder TF. CD19, CD21 and CD22: multifaceted response regulators of B lymphocyte signal transduction. Int Rev Immunol. 2001;20:739-762.
12. Matsumoto AK, Kopicky-Burd J, Carter RH, Tuveson DA, Tedder TF, Fearon DT. Intersection of the complement and immune systems: a signal transduction complex of the B lymphocyte-containing complement receptor type 2 and CD19. J Exp Med. 1991;173:55-64.
13. Botto M, Walport MJ. Hereditary deficiency of C3 in animals and humans. Int Rev Immunol. 1993;10:37-50.
14. Pepys MB. Role of complement in induction of antibody production in vivo. Effect of cobra factor and other C3-reactive agents on thymus-dependent and thymus-independent antibody responses. J Exp Med. 1974;140:126-145.
15. Bitter-Suermann D, Burger R. C3 deficiencies. Curr Top Microbiol Immunol. 1989;153:223-233.
16. Fischer MB, Ma M, Goerg S, et al. Regulation of the B cell response to T-dependent antigens by classical pathway complement. J Immunol. 1996;157:549-556.
17. Wessels MR, Butko P, Ma M, Warren HB, Lage AL, Carroll MC. Studies of group B streptococcal infection in mice deficient in complement component C3 or C4 demonstrate an essential role for complement in both innate and acquired immunity. Proc Natl Acad Sci U S A. 1995;92:11490-11494.
18. Guinamard R, Okigaki M, Schlessinger J, Ravetch J. Absence of marginal zone B cells in Pyk-2-deficient mice defines their role in the humoral response. Nat Immunol. 2000;1:31-36.
19. Ochsenbein AF, Pinschewer DD, Odermatt B, Carroll MC, Hengartner H, Zinkernagel RM. Protective T cell-independent antiviral antibody responses are dependent on complement. J Exp Med. 1999;190:1165-1174.
20. Fischer MB, Goerg S, Shen L, et al. Dependence of germinal center B cells on expression of CD21/CD35 for survival. Science. 1998;280:582-585.
21. Thornton BP, Vetvicka V, Ross GD. Natural antibody and complement-mediated antigen processing and presentation by B lymphocytes. J Immunol. 1994;152:1727-1737.
22. Dempsey PW, Allison MED, Akkaraju S, Goodnow CC, Fearon DT. C3d of complement as a molecular adjuvant: bridging innate and acquired immunity. Science. 1996;271:348-350.
23. Carter RH, Fearon DT. CD19: lowering the threshold for antigen receptor stimulation of B lymphocytes. Science. 1992;256:105-107.
24. Carter RH, Spycher MO, Ng YC, Hoffman R, Fearon DT. Synergistic interaction between complement receptor type 2 and membrane IgM on B lymphocytes. J Immunol. 1988;141:457-463.
25. Tooze RM, Doody GM, Fearon DT. Counterregualtion by the coreceptors CD19 and CD22 of MAP kinase activation by membrane immunoglobulin. Immunity. 1997;7:59-67.
26. Chalupny NJ, Kanner SB, Schieven GL, et al. Tyrosine phosphorylation of CD19 in pre-B and mature B cells. EMBO J. 1993;12:2691-2696.
27. Krop I, Shaffer AL, Fearon DT, Schlissel MS. The signaling activity of murine CD19 is regulated during cell development. J Immunol. 1996;157:48-56.
28. Uckun FM, Burkhardt AL, Jarvis L, et al. Signal transduction through the CD19 receptor during discrete developmental stages of human B-cell ontogeny. J Biol Chem. 1993;268:21172-21184.
29. Wang Y, Brooks SR, Li X, et al. The physiologic role of CD19 cytoplasmic tyrosines. Immunity. 2002;17:501-514.
30. Buhl AM, Cambier JC. Phosphorylation of CD19 Y484 and Y515, and linked activation of phosphatidylinositol 3-kinase, are required for B cell antigen receptor-mediated activation of Bruton's tyrosine kinase. J Immunol. 1999;162:4438-4446.

31. Fujimoto M, Fujimoto Y, Poe JC, et al. CD19 regulates src family protein tyrosine kinase activation in B lymphocytes through processive amplification. Immunity. 2000;13:47-57.
32. Nutt SL, Heavey B, Rolink AG, Busslinger M. Commitment of the B-lymphoid lineage depends on the transcription factor Pax5. Nature. 1999; 401:556-562.
33. Max EE, Wakatsuki Y, Neurath MF, Strober W. The role of BSAP in immunoglobulin isotype switching and B-cell proliferation. Curr Top Microbiol Immunol. 1995;194:449-458.
34. Ohshima Y, Tanaka Y, Tozawa H, Takahashi Y, Maliszewski C, Delespesse G. Expression and function of OX40 ligand on human dendritic cells. J Immunol. 1997;159:3838-3848.
35. Azuma M, Cayabyab M, Phillips JH, Lanier LL. Requirements for CD28-dependent T cell-mediated cytotoxicity. J Immunol. 1993;150:2091-2101.
36. Karasuyama H, Kudo A, Melchers F. The proteins encoded by the VpreB and lambda 5 pre-B cell-specific genes can associate with each other and with mu heavy chain. J Exp Med. 1990;172:969-972.
37. Morimoto S, Kanno Y, Tanaka Y, et al. CD134L engagement enhances human B cell Ig production: CD154/CD40, CD70/CD27, and CD134/CD134L interactions coordinately regulate T cell-dependent B cell responses. J Immunol. 2000; 164:4097-4104.
38. Schneider P, MacKay F, Steiner V, et al. BAFF, a novel ligand of the tumor necrosis factor family, stimulates B cell growth. J Exp Med. 1999;189: 1747-1756.
39. Litinskiy MB, Nardelli B, Hilbert DM, et al. DCs induce CD40-independent immunoglobulin class switching through BLyS and APRIL. Nat Immunol. 2002;3:822-829.
40. Kehrl JH, Riva A, Wilson GL, Thevenin C. Molecular mechanisms regulating CD19, CD20 and CD22 gene expression. Immunol Today. 1994;15: 432-436.
41. Scapini P, Nardelli B, Nadall G, et al. G-CSF-stimulated neutrophils are a prominent source of functional BLyS. J Exp Med. 2003;197:297-302.
42. Wakatsuki Y, Neurath MF, Max EE, Strober W. The B cell-specific transcription factor BSAP regulates B cell proliferation. J Exp Med. 1994; 179:1099-1108.
43. Horcher M, Souabni A, Busslinger M. Pax5/BSAP maintains the identity of B cells in late B lymphopoiesis. Immunity. 2001;14:779-790.
44. Niiro H, Clark EA. Regulation of B-cell fate by antigen-receptor signals. Nat Rev Immunol. 2002;2: 945-956.
45. Seshasayee D, Valdez P, Yan M, Dixit VM, Tumas D, Grewal IS. Loss of TACI causes fatal lymphoproliferation and autoimmunity, establishing TACI as an inhibitory BLyS receptor. Immunity. 2003; 18:279-288.
46. Schebesta M, Pfeffer PL, Busslinger M. Control of pre-BCR signaling by Pax5-dependent activation of the BLNK gene. Immunity. 2002;17:473-485.
47. Ren CL, Morio T, Fu SM, Geha RS. Signal transduction via CD40 involves activation of lyn kinase and phosphatidylinositol-3-kinase, and phosphorylation of phospholipase C gamma 2. J Exp Med. 1994;179:673-680.
48. Breitfeld D, Ohl L, Kremmer E, et al. Follicular B helper T cells express CXC chemokine receptor 5, localize to B cell follicles, and support immunoglobulin production. J Exp Med. 2000;192:1545-1552.
49. Xu J, Foy TM, Laman JD, et al. Mice deficient for the CD40 ligand. Immunity. 1994;1:423-431.
50. Renshaw BR, Fanslow WC, Armitage RJ, et al. Humoral immune responses in CD40 ligand-deficient mice. J Exp Med. 1994;180:1889-1990.
51. Muramatsu M, Kinoshita K, Fagarasan S, Yamada S, Shinkai Y, Honjo T. Class switch recombination and hypermutation require activation-induced cytidine deaminase (AID), a potential RNA editing enzyme. Cell. 2000;102:553-563.
52. Marquart HV, Svendsen A, Rasmussen JM, et al. Complement receptor expression and activation of the complement cascade on B lymphocytes from patients with systemic lupus erythematosus (SLE). Clin Exp Immunol. 1995;101:60-65.
53. Takahashi K, Kozono Y, Waldschmidt TJ, et al. Mouse complement receptors type 1 (CR1; CD35) and type 2 (CR2; CD21): expression on normal B subpopulations and decreased levels during the development of autoimmunity in MRL/lpr mice. J Immunol. 1997;159:1557-1569.
54. Tedder TF, Inaoki M, Sato S. The CD19-CD21 complex regulates signal transduction thresholds governing humoral immunity and autoimmunity. Immunity. 1997;6:107-118.
55. Sato S, Hasegawa M, Fujimoto M, Tedder TF, Takehara K. Quantitative genetic variation in CD19 expression correlates with autoimmunity. J Immunol. 2000;165:6635-6643.
56. Gross JA, Johnston J, Mudri S, et al. TACI and BCMA are receptors for a TNF homologue implicated in B-cell autoimmune disease. Nature. 2000;404:995-999.

Crucial Role of Inhibitor of DNA Binding/Differentiation in the Vascular Endothelial Growth Factor-Induced Activation and Angiogenic Processes of Human Endothelial Cells[1]

Daisuke Sakurai,*¶ Naoyuki Tsuchiya,[2]* Akihiro Yamaguchi,† Yurai Okaji,‡ Nelson H. Tsuno,§ Tetsuji Kobata,¶ Koki Takahashi,§ and Katsushi Tokunaga*

Angiogenesis plays a pivotal role in the aggressive proliferation of synovial cells in rheumatoid arthritis. We have previously reported the overexpression of inhibitor of DNA binding/differentiation (Id) in the endothelial cells within the synovial tissues of rheumatoid arthritis. In this study, we investigated the role of Id in inflammation and angiogenesis in an in vitro model using HUVECs. Vascular endothelial growth factor (VEGF) and TGFβ induced the expression of Id1 and Id3 in HUVECs. Forced expression of Id induced proliferative activity in HUVECs accompanied by down-regulation of $p16^{INK4a}$. Overexpression of Id enhanced expression of ICAM-1 and E-selectin, and induced angiogenic processes such as transmigration, matrix metalloproteinase-2 and -9 expression, and tube formation. In contrast, knockdown of Id1 and Id3 with RNA interference abolished proliferation, activation, and angiogenic processes of HUVECs induced by VEGF. These results indicated that Id plays a crucial role in VEGF-induced signals of endothelial cells by causing activation and potentiation of angiogenic processes. Based on these findings, it was proposed that inhibition of expression and/or function of Id1 and Id3 may potentially be of therapeutic value for conditions associated with pathological angiogenesis. ***The Journal of Immunology*****, 2004, 173: 5801–5809.**

Angiogenesis (1), along with recruitment of inflammatory cells, production of proinflammatory cytokines (2), and aggressive proliferation of fibroblast-like synoviocytes (3), is critically involved in the process of chronic inflammation and joint destruction in rheumatoid arthritis (RA).[3] In the previous study, through a comprehensive analysis of mRNA in the synovial tissues, we identified overexpression of inhibitor of DNA binding/differentiation (Id) family proteins, Id1 and Id3, and their localization to the endothelial cells, within the synovial tissues of RA (4).

The Id family consists of four members, Id1 to Id4, which contain helix-loop-helix (HLH) domains, but not DNA binding domains (5). Id proteins were originally identified as dominant-negative antagonists of the basic HLH transcription factors such as MyoD (5) as well as non-basic HLH proteins such as Rb (6), and have been known to play a crucial role in developmental processes (7–11). They are predominantly expressed in fetal tissues and in some transformed cells (12), and are down-regulated during differentiation (13, 14). Id also controls cell proliferation and the progression of cell cycle (15). Id has been shown to repress $p16^{INK4a}$ expression by directly inhibiting the binding of Ets1 and Ets2 transcription factors to $p16^{INK4a}$ promoter (16), and to prevent exit from the cell cycle. Expression of Id3 is regulated by Ras-ERK MAPK cascade (17) and Smad1/5 signaling (18).

A previously unsuspected role of Id was recently disclosed. $Id1^{+/-}$ $Id3^{-/-}$ mice were unable to support angiogenesis necessary for the progression of tumor xenografts (19), suggesting that Id1 and Id3 may also be required for the angiogenesis in adult tissues. We hypothesized that the localization of Id within the synovial endothelial cells in RA (4) may imply involvement of Id in the inflammation and angiogenesis typically observed in the synovial tissues of RA. If this is the case, Id can be an attractive target for the treatment not only of cancer, but also of RA, because expression of Id is usually weak in normal adult tissues, except for the proliferating cells (20).

In the present study, we examined whether the overexpression of Id alone can induce activation and angiogenesis in cultured human endothelial cells, and whether suppression of Id can inhibit activation and angiogenic processes of these cells induced by vascular endothelial growth factor (VEGF).

Materials and Methods

Monoclonal Abs

The mAbs used for flow cytometry were as follows: FITC-labeled anti-human α_v integrin (Beckman Coulter, Fullerton, CA), PE-labeled anti-human ICAM-1 (Beckman Coulter), PE-labeled anti-human β_1 integrin (DakoCytomation, Carpinteria, CA), CyChrome-labeled anti-human E-selectin (BD Biosciences, San Jose, CA), and unlabeled anti-human α_2 integrin (DakoCytomation). MsIgG1-RD1/MsIgG1-FITC (Beckman Coulter), IgG1-PE (Beckman Coulter), IgG1-CyChrome (BD Biosciences), and unlabeled IgG1 (DakoCytomation) were used as isotype controls.

Endothelial cell culture and transient transfection

Primary HUVECs were isolated as previously described (21) and cultured in MCDB151 medium (Sigma-Aldrich, St. Louis, MO) supplemented with

Departments of *Human Genetics, †Allergy and Rheumatology, ‡Surgical Oncology, and §Transfusion Medicine, Graduate School of Medicine, University of Tokyo, Tokyo, Japan; and ¶Division of Immunology, Institute for Medical Science, Dokkyo University School of Medicine, Tochigi, Japan

Received for publication March 16, 2004. Accepted for publication August 26, 2004.

The costs of publication of this article were defrayed in part by the payment of page charges. This article must therefore be hereby marked *advertisement* in accordance with 18 U.S.C. Section 1734 solely to indicate this fact.

[1] This work was supported by Grant-in-Aid for Scientific Research on Priority Areas (C) "Medical Genome Science," and Grant-in-Aid for Scientific Research (B) from the Ministry of Education, Science, Sports and Culture of Japan, and by Health and Labour Sciences Research Grant for Research on Allergic Disease and Immunology from the Ministry of Health Labour and Welfare of Japan.

[2] Address correspondence and reprint requests to Dr. Naoyuki Tsuchiya, Department of Human Genetics, Graduate School of Medicine, University of Tokyo, 7-3-1 Hongo, Bunkyo-ku, Tokyo, Japan 113-0033. E-mail address: tsuchiya-tky@umin.ac.jp

[3] Abbreviations used in this paper: RA, rheumatoid arthritis; Id, inhibitor of DNA binding/differentiation; HLH, helix-loop-helix; VEGF, vascular endothelial growth factor; FGF, fibroblast growth factor; bFGF, basic FGF; shRNA, small hairpin RNA; MMP, matrix metalloproteinase; RNAi, RNA interference.

0022-1767/04/$02.00